Optical phenomena in thin-film waveguides

E. M. Zolotov, V. A. Kiselev, and V. A. Sychugov

P. N. Lebedev Physics Institute, USSR Academy of Sciences
Usp. Fiz. Nauk 112, 231–273 (February 1974)

The review reflects the results of theoretical and experimental investigations of thin dielectric films with an aim of using them to develop integrated optical circuits. The principal properties of optical waveguides on dielectric substrates are considered. Methods are analyzed for the admission and extraction of light through the waveguide surface using the optical tunnel effect, using a phase diffraction grating, and using a gradually tapering edge. Attention is paid to the conversion of the frequency of laser radiation in a nonlinear thin-film waveguide, and also to the losses due to absorption and scattering of light in the films. The review describes, in addition, the principal results of theoretical and experimental research on the interaction of optical and acoustic waves in thin films, and on amplification and generation of light in activated thin-film waveguides. Passive optical elements based on thin films are also considered.

CONTENTS

INTRODUCTION

Quantum electronics has recently reached a development level such that its capabilities, discovered in laboratory research, are finding ever increasing practical applications. In particular, the use of thin-film dielectric waveguides uncovers a way of producing miniature laser devices, optical modulators, filters, parametric generators, and other elements for communication systems with large information capacity, high-speed computing devices, and systems of optical information processing. The formation of thin-film optical elements on flat dielectric substrates will make it possible in the future to construct integrated optical circuits which are insensitive to external (thermal and mechanical) influences, are economical in operation, and are cheap when produced on a commercial scale. These prospects stimulated a new field of research at the junction of microwave engineering and optics, namely integrated optics. The first work on flat asymmetrical dielectric waveguides with thickness on the order of the light wavelength were performed in our country in 1967–1968 [1-3]. These consisted of studies of the principal properties of optical waveguides on dielectric substrates, development of a method for the entry and exit of the light through the waveguide surface by using the tunnel effect, and conversion of laser-emission frequency in a nonlinear thin-film waveguide. Following the publication of [4,5], where different variants of the utilization of optical waveguides and integrated circuits were proposed, extensive integrated-optics research has developed abroad. By now, considerable progress has been reached in this field. The dispersion characteristics of asymmetrical dielectric waveguides, and also the field distribution and the light fluxes produced in them by surface waves have been quite fully investigated theoretically and experimentally [1,6-17] (see Chap. 1). By using thin-film waveguides of varying optical thickness, passive optical elements were developed such as lenses, prisms, and diffraction gratings [6,18-21] (see Chap. 2). Entry of radiation via the tunnel effect[2,6,8,21-31], effective methods of exciting a definite surface wave through a gradually narrowing edge of a waveguide film and through a three-dimensional (or planar) phase diffraction grating deposited directly on its surface were developed [2,11,32-41] (see Chap. 3). Calculations and measurements were made of the optical losses due to absorption and scattering by inhomogeneities in a real film, and also due to noticeable scattering by its optically imperfect and rough walls [1,2,7,11,16,17,42-46].

The possibility of obtaining light fluxes of high density over sufficiently extended sections of a thin-film waveguide is its main advantage when various nonlinear interactions are effected between the light waves [2,11,15,29,47-52] (see Chap. 4). In addition, it can be noted that the thin-film waveguides make it possible to use isotropic nonlinear materials and afford new relatively simple possibilities for frequency tuning of parametrically-excited waves [2,15]. Published experimental papers on nonlinear effects in thin films are limited to reports of observation of the second harmonic and of the difference frequency [2,51,52].

In Chap. 5 of this review we present the principal results of theoretical and experimental research on spatial modulation of optical surface waves when they interact with acoustic waves [53-55], and also the results of research on the mutual conversion of surface waves in thin films with anisotropic boundary media [56-58]. The last and sixth chapter is devoted to problems connected with amplification and generation of light in activated thin-film waveguides [59,72].

Confining ourselves to purely physical problems, we do not dwell here on the technology of manufacture of strip thin-film waveguides (width of the order of several wavelengths), although it should be emphasized that the development of such low-loss waveguides is a fundamental practical problem of integrated optics at the present

stage of its development. Intensive searches are therefore being made for new materials, namely organic and inorganic semiconductors and dielectrics[15,43,44,46,73].

In addition to the known methods of obtaining waveguide layers [74-76], new methods are being developed [15,77], particularly those using ion diffusion and penetration of protons into the substrate [78-80]. Circuits comprising strip optical waveguides are produced on a single dielectric substrate not only by photolithography, but also by exposing the photoresist to a laser or electron beam [35,81,82], by engraving the substrate with subsequent filling of the microscopic grooves with polymerizing material [73], and by other methods[15,64,83].

1. PROPAGATION OF LIGHT WAVES IN THIN DIELECTRIC FILMS

A homogeneous dielectric film of constant thickness, deposited on a flat dielectric substrate, constitutes a flat (generally speaking, asymmetrical) optical waveguide if the dielectric constant ϵ_0 of the film exceeds the dielectric constants ϵ_1 and ϵ_2 of the adjacent media.

The field of monochromatic waves (with time dependence $e^{-i\omega t}$) propagating in such a waveguide (Fig. 1) along the x axis and homogeneous along the y axis, is described by the two-dimensional scalar wave equation

$$\left(\frac{\partial^2}{\partial x^2}+\frac{\partial^2}{\partial z^2}+k_j^2\right)v(x,z)=0, \tag{1.1}$$

where $k_j = n_j k$, $k = \omega/c$ is the wave number in vacuum, $n_j = \sqrt{\epsilon_j}$ stands for the refractive indices of the media ($j = 0, 1, 2$), the absorption of light in which we neglect. Depending on the two possible polarizations of the light in the waveguide, the wave function v coincides either with the electric field vector

$$v = E_y \quad \text{и} \quad H_x = \frac{ic}{\omega}\frac{\partial v}{\partial z}, \qquad H_z = -\frac{ic}{\omega}\frac{\partial v}{\partial x} \quad (H\text{-waves}), \tag{1.2}$$

or with the magnetic vector

$$v = H_y \quad \text{и} \quad E_x = -\frac{ic}{\omega\varepsilon}\frac{\partial v}{\partial z}, \qquad E_z = \frac{ic}{\omega\varepsilon}\frac{\partial v}{\partial x} \quad (E\text{-waves}) \tag{1.3}$$

(see [84]). To satisfy the boundary conditions on the planes $z = 0$ and $z = -h$, which separate the dielectric layers, the waves $v(x, z)$ should be represented in the form $Z(z)X(x)$, i.e., in the form of plane waves

$$v(x,z)=Z(z)X(x)=[C_j^+\exp(ik_j\cos\theta_j\cdot z) + C_j^-\exp(-ik_j\cos\theta_j\cdot z)]\exp(ik_j\sin\theta_j\cdot x), \quad C_j^{\pm}=\text{const}. \tag{1.4}$$

The constants θ_j which result from the separation of the variables in the wave equation, specify the angles, relative to the z axis, at which the incident and reflected plane waves $\exp[i(k_{jx}x \pm k_{jz}z - \omega t)]$ propagate in each of the media. By virtue of the continuity of the field on the surfaces separating the dielectrics ($z = 0, -h$),

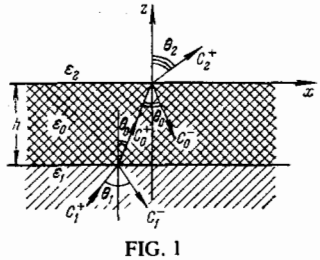

FIG. 1

these waves should have the same dependence on the coordinate x:

$$k_{jx} = \text{const} = k_x = n^*k \quad \text{или} \quad n_0\sin\theta_0 = n_1\sin\theta_1 = n_2\sin\theta_2 = n^*. \tag{1.5}$$

In other words, the wave propagation direction should satisfy the law of refraction (and reflection) of light. Further analysis of the continuity of the tangential components of the field for the two boundary values $z(0, -h)$ makes it possible to obtain, on the basis of (1.4), the field distributions that are possible in the three-layer dielectric media considered by us. We shall dwell on them in greater detail later on, and for the time being we discuss the detailed boundary condition (1.5). Since, by assumption, $n_2 < n_1$ and n_0, it follows that when the angle of inclination θ_0 of the wave vector k_0 is increased the angle θ_2 will be the first to reach the limiting real value $\pi/2$. Of course, the condition (1.5) remains in force at $n^* > n_2$ (or $k_x > k_2$), but then real angles θ_0 will correspond to imaginary values of the constant θ_2. Introducing in its place a new constant for the second medium in accordance with the formula $\alpha_2 = i[\theta_2 - (\pi/2)]$, we obtain $n_2\sin\theta_2 = n_2\cosh\alpha_2$ for the condition (1.5) and $ik_2\cos\theta_2 = -k_2\sinh\alpha_2$ for relation (1.4). When $k_x > k_2$, the parameter α_2 assumes real values under the condition (1.5). According to (1.4), the field in the second medium decreases exponentially with increasing distance from the interface $z = 0$. There is no field increasing exponentially along the z axis in the second medium ($C_2^- = 0$) if no radiation enters the dielectric film from this medium (see Chap. 3). Thus, if $k_x > k_2$ the light wave travels in the second medium along the boundary surface, and the light propagating in the film experiences total internal reflection from this boundary surface.

As the angle of incidence of the wave on the walls of the dielectric film is increased further, the parameter n^* eventually becomes larger than the refractive index n_1 of the substrate. The wave propagating in the film is then totally reflected from both boundary media. The field penetrating into the first and into the second medium decreases exponentially with increasing distance from the film. Thus, under the condition

$$n_0 \geqslant n^* > n_1 \ (\text{and } n_2) \tag{1.6}$$

the optical radiation becomes channeled in the dielectric waveguide and the so-called surface waves are produced and travel along the film. The propagation velocity of the surface waves, $v_x = \omega/k_x = c/n^*$ is smaller than the light velocities $v_{1,2} = c/n_{1,2}$ in the first and second media, but is larger than the light velocity $v_0 = c/n_0$ in the film. We note that the parameter n^*, which was introduced together with the incidence angle θ_0, plays the role of the effective refractive index for the given surface wave, and the values of this index cannot go beyond the limits indicated in (1.6). We introduce next for the first medium (as was done previously for the second medium) the real parameter α_1 instead of the imaginary constant θ_1, rewrite the boundary condition (1.5) in the form

$$n^* = n_0\sin\theta_0 = n_1\operatorname{ch}\alpha_1 = n_2\operatorname{ch}\alpha_2 \tag{1.7}$$

and make the substitutions

$$ik_j\sin\theta_j = in^*k, \quad ik_0\cos\theta_0 = ik\sqrt{n_0^2-n^{*2}}, \quad ik_{1,2}\cos\theta_{1,2} = -k\sqrt{n^{*2}-n_{1,2}^2} \tag{1.8}$$

in (1.4). It is also necessary to put in (1.4), in the absence of optical pumping from either medium, $C_1^+ = C_2^- = 0$.

On the basis of the continuity of the tangential field components, at the interface between the film and the second medium (z = 0), we can express the amplitudes C_0^- and C_2^+ of the reflected wave and of the wave penetrating into the second medium in terms of the amplitude C_0^+ of the incident wave (see formulas (1.16) below). In the case of total internal reflection, the amplitudes C_0^+ and C_0^- are naturally equal in magnitude:

$$C_0^-/C_0^+ = \exp(-i\delta_{02}), \tag{1.9}$$

and the phase shift between them is [4]

$$\delta_{02} = 2\operatorname{arctg}\left[\sqrt{\frac{n^{*2}-n_2^2}{n_0^2-n^{*2}}}\left(\frac{n_0}{n_2}\right)^{\varkappa}\right], \quad \varkappa = \frac{2H_y}{H}, \tag{1.10}$$

where $H_y = 0$ in the case of the H waves (1.2) and $H = H_y$ in the case of the E waves (1.3).

By satisfying analogous conditions on the boundary z = −h between the film and the first medium we can obtain with the aid of (1.4) the amplitude C_1^- of the wave penetrating into this medium (more accurately, C_1^-/C_0^-), and show that

$$\frac{C_0^+}{C_0^-}\exp(-2ik_0h\cos\theta_0) = \exp(-i\delta_{01}), \tag{1.11}$$

where the phase shift δ_{01} corresponding to total internal reflection from the surface of the first medium is described by formula (1.10) in which n_2 is replaced by n_1. It is easily seen that Eqs. (1.9) and (1.11) are compatible if

$$2k_0\cos\theta_0 \cdot h - \delta_{01} - \delta_{02} = 2\pi(m-1), \tag{1.12}$$

or

$$kh\sqrt{n_0^2-n^{*2}} = \tag{1.13}$$
$$= \pi(m-1) + \operatorname{arctg}\left(\frac{n_0}{n_1}\right)^{\varkappa}\sqrt{\frac{n^{*2}-n_1^2}{n_0^2-n^{*2}}} + \operatorname{arctg}\left(\frac{n_0}{n_2}\right)^{\varkappa}\sqrt{\frac{n^{*2}-n_2^2}{n_0^2-n^{*2}}},$$

where m = 1, 2, 3, ... Thus, a monochromatic light wave can propagate in a dielectric film via total reflections from its walls only at definite incidence angles θ_{0m} that follow from the condition (1.12). These angles θ_{0m} decrease with increasing m, and the minimal angle of incidence $\theta_{0\tilde{m}}$ (or the possible number $\tilde{m}$ of surface waves of frequency ω in the given dielectric waveguide) is determined by the lower limit (n_1) of the effective refractive index n^* of the surface waves:

$$n_0\sin\theta_{0m} > n_1 \qquad (m = 1, 2, \ldots, \tilde{m}). \tag{1.14}$$

On the other hand, if we fix the value of m, then relation (1.13) assumes the role of a dispersion equation that describes the dependence of the effective refractive index n_m^* of the given surface wave on its frequency ω. The effective refractive index n_m^* depends also on the thickness h of the dielectric film, a fact used to produce passive optical elements (prisms and lenses) that act on surface waves in the (x,y) plane of the waveguide (see Chap. 2). As n_m approaches its lower limit n_1 (i.e., with decreasing angle of incidence θ_{0m}), the quantity kh in (1.13) reaches its minimal permissible value

$$(kh)_{\min} = (n_0^2-n_1^2)^{-1/2}\left[\pi(m-1) + \operatorname{arctg}\left(\frac{n_0}{n_2}\right)^{\varkappa}\sqrt{\frac{n_1^2-n_2^2}{n_0^2-n_1^2}}\right], \quad k = \frac{\omega}{c}. \tag{1.15}$$

In a dielectric film of given thickness h, relation (1.15) determines the critical frequency $\omega_m^{\min}$ for each of the surface waves. If the light frequency ω becomes less than the critical frequency, then the surface wave goes over into a wave that does not experience total internal reflection, at least on the interface of the film and the first medium, so that light starts to be emitted from the surface of the waveguide into this medium. For this reason, in order for the m-th surface wave at the frequency ω to exist, the thickness of the dielectric film should exceed the critical thickness $h_m^{\min}$ that follows from (1.15). Since the phase shift of the E wave is larger in the case of total internal reflection than the phase shift of the H wave, the critical thickness of the film turns out to be larger for the first of the indicated polarizations of the m-th surface wave: $h_{E,m}^{\min} > h_{H,m}^{\min}$. When m is increased by unity, the critical thickness of the film invariably increases by $\lambda/2\sqrt{n_0^2-n_1^2}$. Using a film of suitable thickness, we can limit the number of surface waves of the dielectric waveguide at will (in particular, to one wave H_1).

According to (1.13), analogous relations between the relative film thicknesses kh corresponding to E_m and H_m waves hold true for any fixed value of n^*. By way of illustration, Fig. 2 shows the dependence of the effective refractive indices n_m^* on the relative film thickness for surface E_m and H_m waves of low order, for material refractive indices $n_0 \approx 4.0$, $n_1 \approx 1.42$ and $n_2 = 1.0$ (a) [1] and for closer values $n_0 = 2.3$, $n_1 = 1.5$, and $n_2 = 1.0$ (b) [11]. The first case (Fig. 2a) describes in the wavelength band $\lambda = 2$–$4\ \mu$, a germanium film deposited on a quartz substrate and in contact with air on the other side. The second case (Fig. 2b) corresponds in the vicinity of $\lambda \sim 1\ \mu$ to a film of ZnS on a glass substrate in air.

In any longitudinal plane z = const of the waveguide shown in Fig. 1, its surface waves are traveling waves of the type $\exp[i(n^*kx - \omega t)]$. In a transverse plane x = const inside the film ($0 \geq z \geq -h$), the light field is described by the standing wave $C_0^+e^{-i\omega t}\{\exp(i\sqrt{n_0^2-n^{*2}}kz) + \exp[-i(\sqrt{n_0^2-n^{*2}}kz + \delta_{02})]\}$, which is produced as a result of a superposition of the wave incident on the film wall and the wave reflected from it. At an incidence angle $\theta_{0m}(n_m^* = n_0\sin\theta_m)$, i.e., in the case of a surface wave with index m, the standing wave has (m − 1) nodes. On the whole, the surface-wave field is distributed in the following manner:

$$v(x, z, t) = Z(z)\exp[i(n^*kx - \omega t)],$$
$$Z(z) = \tag{1.16}$$
$$= \begin{cases} C_2^+\exp(-\sqrt{n^{*2}-n_2^2}kz), & z \geqslant 0, \\ 2\exp(-i\delta_{02}/2)\,C_0^+\cos\left[\sqrt{n_0^2-n^{*2}}kz + \frac{1}{2}\delta_{02}(n^*)\right], & 0 \geqslant z \geqslant -h, \\ C_1^-\exp(\sqrt{n^{*2}-n_1^2}kz), & z \leqslant -h, \end{cases}$$

where the amplitudes of the waves penetrating into the first and second media are $C_2^+ = 2C_0^+/[1 + i\tan(\delta_{02}/2)]$, $C_1^- = 2C_0^+\exp[(\sqrt{n^{*2}-n_1^2} - i\sqrt{n_0^2-n^{*2}})kh]/[1 - i\tan(\delta_{01}/2)]$; $\tan(\delta_{02(01)}/2)$ is defined in (1.10). The magnetic field of the H_m waves ($v = E_y$) and the electric field of the E_m waves ($v = H_y$) can be easily calculated from for-

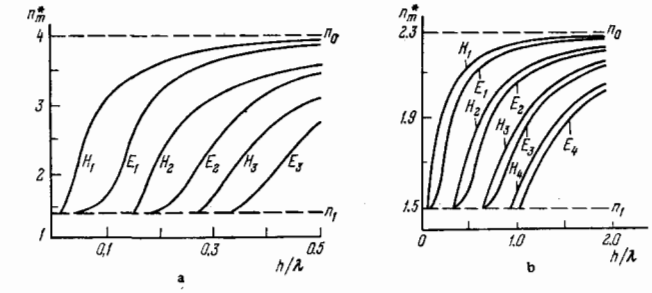

FIG. 2

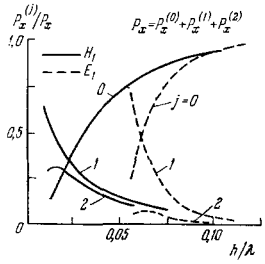

FIG. 3

mulas (1.2) and (1.3), respectively. The resultant expressions are given in [11].

The time-averaged energy flux carried by the surface wave along the thin-film waveguide in each of the constituent media (through a section of unit width along the y axis) is given by the general expression

$$P_x^{(j)}=\int dz\left[\frac{1}{2\pi}\int_{-\pi}^{\pi}S_x^{(j)}\,d(\omega t)\right]=\frac{c}{8\pi}\,\mathrm{Re}\int(\bar{E}_yH_z-\bar{E}_zH_y)\,dz=\frac{cn^*}{8\pi n_j^\varkappa}\int|v|^2\,dz\qquad(j=0,\,1,\,2). \tag{1.17}$$

taking into consideration the field distribution (1.16), we get

$$P_x^{(0)}=(cn^*\,|\,C_0^+\,|^2/4\pi n_0^\varkappa)\,\{h+[(\sin\delta_{01}+\sin\delta_{02})/2k\sqrt{n_0^2-n^{*2}}]\},$$
$$P_x^{(1,2)}=cn^*\,|\,C_0^+\,|^2(1+\cos\delta_{01,\,02})/8\pi n_{1,2}^\varkappa k\sqrt{n^{*2}-n_{1,2}^2}. \tag{1.18}$$

Similar formulas are given in [11]. The results of the calculation performed in that reference for a germanium film on a quartz substrate ($n_0\approx 4.0$, $n_1\approx 1.42$, $n_2=1.0$) are shown in Fig. 3. We see that at a relative film thickness close to critical for the E_1 wave (see Fig. 2a) the greater part of the H_1-wave energy is carried in the interior of the film. With further decrease of the film thickness the field of the fundamental surface wave (and the radiation flux produced by the wave) becomes distributed to an ever increasing degree in the neighboring media, especially in the substrate. This behavior is typical of all surface waves and follows directly from the general uncertainty relation $\Delta k_z\cdot\Delta z\gtrsim 1$.

The total energy flux produced by the surface wave is conveniently expressed in the form

$$P_x=\frac{1}{2}S_{\max}^{(0)}h^*, \tag{1.19}$$

where $S_{\max}^{(0)}$ denotes the maximum density of the time-averaged light flux in the film:

$$S_{\max}^{(0)}=cn^*\,|\,C_0^+\,|^2/2\pi n_0^\varkappa \tag{1.20}$$

(see relations (1.17) and (1.16)), and h* denotes the effective thickness of the waveguide, over which the total energy flux becomes distributed with an average density $S_{\max}^{(0)}/2$:

$$kh^*=kh+[(\sin\delta_{01}+\sin\delta_{02})/2\sqrt{n_0^2-n^{*2}}]+(n_0/n_1)^\varkappa[(1+\cos\delta_{01})/2\sqrt{n^{*2}-n_1^2}]+(n_0/n_2)^\varkappa[(1+\cos\delta_{02})/2\sqrt{n^{*2}-n_2^2}]. \tag{1.21}$$

Expanding $\delta_{02(01)}$ in accordance with formula (1.10), we obtain

$$kh^*=kh+(n^{*2}-n_1^2)^{-1/2}\left[\left(\frac{n^*}{n_0}\right)^\varkappa+\left(\frac{n^*}{n_1}\right)^\varkappa-1\right]^{-1}+(n^{*2}-n_2^2)^{-1/2}\left[\left(\frac{n^*}{n_0}\right)^\varkappa+\left(\frac{n^*}{n_2}\right)^\varkappa-1\right]^{-1}, \tag{1.22a}$$

where $\varkappa=2H_y/H$. In the case of H waves ($\varkappa=0$), the last formula becomes much simpler

$$kh^*=kh+(n^{*2}-n_1^2)^{-1/2}+(n^{*2}-n_2^2)^{-1/2}. \tag{1.22b}$$

We see that at a fixed value of n* the effective waveguide thickness h* exceeds the film thickness h by the same amount for all E_m waves ($\varkappa=2$), and by a somewhat different amount for all H_m waves ($\varkappa=0$), m = 1, 2, 3, ... The difference (h* − h) reaches a minimum as $n^*\to n_0$ and increases without limit as $n^*\to n_1$. Fig. 4 shows plots of h* (and h) against the effective refractive index for the case of H_1 and H_2 waves in a ZnS film on a glass substrate ($n_0=2.3$, $n_1=1.5$, $n_2=1.0$; see also Fig. 2b).[11] Similar curves can be easily constructed for H waves of higher order m, if it is recognized that, according to the dispersion equation (1.13) when m is increased by unity the relative film thickness kh (and consequently also kh*) is invariably increased by $\pi(n_0^2-n^{*2})^{-1/2}$:

$$h_{m+1}(n^*)-h_m(n^*)=h_{m+1}^*(n^*)-h_m^*(n^*)=\lambda/2\sqrt{n_0^2-n^{*2}}\qquad(m=1,\,2,\,\ldots), \tag{1.23}$$

where λ is the wavelength of light in vacuum. By choosing the relative film thickness (or n*) and exciting in it the fundamental surface wave H_1, we can obtain the smallest effective thickness $kh_{H,1}^*$ of the waveguide and by the same token (see (1.19)) the largest light-flux density inside the film at a given total flux P_x. In the case represented in Fig. 4, the effective waveguide thickness becomes minimal at a relative film thickness $h_{H,1}/\lambda\approx 0.19$ (and at an effective refractive index $n_{H,1}^*\approx 1.82$). This minimal thickness is $h_{H,1}^*/\lambda\approx 0.435$. For light of wavelength $\lambda\approx 1.06\ \mu$ in vacuum, the effective thickness $h_{H,1}^*$ is 0.46 μ (and $h_{H,1}\approx 0.2\ \mu$). Thus, when a light beam of 1 W power and of 10 μ width (along the y axis) is introduced in the fundamental mode H_1 of a thin-film ZnS waveguide, the average radiation flux density in the film reaches the appreciable value

$$\frac{1}{2}S_{\max}^{(0)}\approx 22\ \mathrm{MW/cm^2},$$

thus producing favorable conditions for the realization of nonlinear interactions (see Chap. 5).

Principal attention will be paid here (and throughout) to surface waves, but in a thin-film waveguide there can be produced in addition waves that do not experience total reflection from the film walls (see the general solution (1.4) at incidence angles θ_0 in the range $0\leq n_0\sin\theta_0=n^*\leq n_1$). In particular, if the film thickness changes in some section of the waveguide, then any surface wave passing through that section is transformed into surface waves of other orders, and also into waves accompanied by radiation of light from the film into the neighboring media. The radiation waves are described in detail in the review [11]. Referring the reader to this review, we recall only that in an asymmetrical dielectric waveguide the radiation waves can be of two types. Namely, in the region $n_2<n^*\leq n_1$ there exists for each

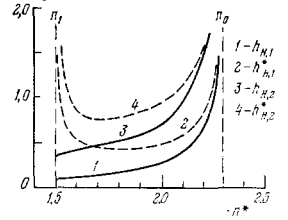

FIG. 4

value of n^* one solution of the type (1.4), which describes a wave incident in the medium, refracted (and partially reflected) in the film, and experiencing total internal reflection from its interface with the second medium. The amplitudes C_1^-, $C_0^\pm$, and C_2^+ of the corresponding waves are expressed in terms of the amplitude C_1^+ of the incident wave with the aid of four boundary conditions. In the region $0 \leq n^* \leq n_2$ there exists for each value of n^*, besides the solution representing the wave incident from the first medium and going through the film off to the second medium, also another independent solution, which describes the propagation of a wave incident on the film from the second medium. In the theory of symmetrical thin-film waveguides it is convenient to use two linear combinations of these solutions, having odd and even field distributions about the z axis, namely $Z_g(z, n^*)$ and $Z_u(z, n^*)$, respectively[16,17]. The convenience lies in the fact that the modes Z_g and Z_u are obviously orthogonal to each other. As to the modes $Z(z, n^*)$ corresponding to different values of the effective refractive index n^*, they are hermitially orthogonal in the general case of an asymmetrical waveguide:

$$\int_{-\infty}^{\infty} Z(z, n^*)\,\bar{Z}(z, n^{*\prime})\,dz = 0 \quad \text{for} \quad n^{*\prime} \neq n^*, \tag{1.24}$$

since they are eigenfunctions of the hermitian linear operator

$$\left[\frac{1}{k^2}\frac{d^2}{dz^2} + n^2(z)\right] Z(z, n^*) = n^{*2} Z(z, n^*), \tag{1.25}$$

where

$$n(z) = \begin{cases} n_2 & \text{for } z > 0, \\ n_0 & \text{for } 0 \geqslant z \geqslant -h, \\ n_1 & \text{for } z < -h. \end{cases}$$

Relation (1.24) holds for both the continuous spectrum of the values $0 \leq n^* \leq n_1$ (radiation waves) and for the discrete spectrum $n_1 < n_m^* \leq n_0$ (surface waves).

We note in conclusion that, confining ourselves to thin-film waveguides on dielectric substrates, we take into account the circumstance that in the far infrared and in the optical bands the radiation losses due to reflection from a metallic substrate (and all the more the losses in hollow metallic waveguides) exceed by several orders of magnitude the losses in films (at the present state of the art of their manufacture) [1,13].

2. PASSIVE OPTICAL ELEMENTS

One of the tasks of integrated optics is the development of passive optical elements (lenses, prisms, diffraction gratings) in a film. This problem can be solved on the basis of the theoretical analysis of the propagation of light in thin waveguide films. In Chap. 1 of this review we described in detail and discussed the fundamental results of this analysis, and have shown in particular that in the region (1.6) of the existence of the mode m its effective refractive index n_m^* increases monotonically with increasing film thickness. This is a fundamental fact for the analysis that follows.

In the case of two-dimensional (film) optics, in volume optics, we can obtain an eikonal equation describing the propagation of a light ray in the film [20]

$$[\operatorname{grad} \varphi(x, y)]^2 = [n^*(x, y)]^2 = N^2(x, y), \tag{2.1}$$

where $\varphi(x,y)$ is the eikonal which determines the phase of the field $v(x, y) = A(x, y)e^{ik\varphi(x,y)}$. The applicability of this equation is limited by the condition $|k \operatorname{grad} N| \ll 1$, which means that the dimensions of the transition from the thin region of the film to the thick one should be much larger than the wavelength of the light. Using the eikonal equation, we can easily derive the law for the refraction of the light on going from one region with $n^* = N^{I}$ to another with $n^* = N^{II}$ [85]:

$$N^{I} \sin \alpha_{I} = N^{II} \sin \alpha_{II}. \tag{2.2}$$

Throughout this chapter, the effect of refractive index of the parts of the film with different frequencies will be designated N^{I}, N^{II}, etc.

It should be noted that the refraction angle α_{II} does not depend on the profile of the thickness of the transition region of the film, but this profile does determine the shift of the ray along the transition boundary, and also the losses to reflection, to radiation, and to mode conversion in the transition region. The snoothness of the transition on the whole minimizes these losses. Refraction of light going from one region of the film with N^{I} to another with N^{II} was observed experimentally in [6,20]. A ZnS film was deposited by vacuum evaporation on a glass substrate. A film of thickness h_I 700 Å was deposited first. Part of the film was then covered by a shield and a second layer was deposited on top of the first. The total thickness of this film layer was $h_{II} \approx 2400$ Å. In the second coating, the covering shield was located at a distance 0.1 mm from the first film layer, making it possible to obtain a smooth transition from one region of the film to the other, with a transition width $L_T \approx 0.05$ mm. A light beam from an He-Ne laser was introduced with the aid of a prism (see Chap. 3) into the film with $h_I = 700$ Å. The authors of [20] verified the validity of Snell's law by measuring the angles α_I and α_{II} and the effective refractive indices N^{I} and N^{II}. Within the limits of the experimental accuracy, which was limited by the errors in the determination of the angles α, no deviations from (2.2) were observed. In this experiment the intensity of the light beam reflected from the transition region was too weak to be registered. The smooth transition from a thin film to a thicker one, with dimensions L_T much larger than the light wavelength λ, has an exceedingly small reflection coefficient $\sim(2\pi N L_T/\lambda)^{-2}$ and is equivalent to the effective nonreflecting coating used in ordinary optics. An exception is the case of total internal reflection, when the light beam propagating in the film region with thickness h_{II} is incident on the transition region at a sufficiently large angle α_{II}^i ($\alpha_{II}^i > \alpha_{cr}$, where $\alpha_{cr} = \sin^{-1}(N^{I}/N^{II})$). The total internal reflection of the ray in the film in the region of the transition is a direct consequence of the refraction law. A light ray reflected from the interface between regions I and II propagates in region II at an angle α_{II}^r to the normal to the interface; this angle is connected with the incidence angle α_{II}^i by the relation

$$\alpha_{II}^r = \pi - \alpha_{II}^i. \tag{2.3}$$

Total internal reflection of light in a thin-film waveguide was observed experimentally by the authors of the cited papers [20,32] at ray incidence angles exceeding the critical value $\alpha_{cr} = 51°$ ($h_I = 700$ Å, $h_{II} = 2400$ Å, ZnS). Obviously, total internal reflection can occur also when the film thickness in region I is less than critical, i.e., $h_I < h^{min}$. In this case the necessary and sufficient condition for total internal reflection is the inequality

$$\alpha_{II}^{i} > \arcsin(n_1/N_{II}). \qquad (2.4)$$

At smaller incidence angles, the light cannot propagate in region I, and is radiated into the substrate from the section with variable thickness. We note that the total internal reflection on the boundary of two regions of the film is actually total in the case of a strictly straight-line boundary.

Just as in ordinary optics, prisms and lens are produced by suitable shaping of the surfaces of dielectric transparent media, in thin films it is possible to produce elements acting as prisms and lenses by suitable shaping of the boundaries of the region where the refractive index N varies. Obviously, this can be primarily effected by varying the film thickness. If we wish to operate with a film in which the fundamental mode propagates, then its thickness should not exceed the critical thickness for the second mode m = 2. The maximum change of the refractive index does not exceed $n_0 - n_1$ in this case:

$$\Delta N_{max} \approx n_0 - n_1.$$

Numerical calculations [21] show that for a film with $n_0 = 1.75$ on a glass substrate in air, it is possible to achieve changes $\Delta N_{max} \approx 0.17$ of the effective refractive index by varying the thickness from 0.2 λ to 0.8 λ. Thin films having large refractive indices, such as CeO_2, ZnS, ZnO, having $n_0 = 2-2.5$, can obviously ensure appreciable changes ΔN, on the order of 0.5 and more. A major shortcoming of these films, however, is the large scattering loss, which limits the propagation of light in them to distances up to several (1–3) centimeters and makes their use as waveguides difficult. It is therefore proposed in [21] to produce prisms and lenses by introducing a suitably shaped layer with high refractive index into the waveguide film or the substrate, as shown in Fig. 5.

Prisms and lenses based on films were experimentally investigated in [6,20]. In one of these studies [6] the prism was a rectangular film region with larger thickness. The light beam propagating in the film was refracted both on entering and on leaving the film. The angle φ of the beam deflection by the prism and the prism dispersion $\partial\varphi/\partial\lambda$ could be calculated from the standard formulas for three-dimensional prisms, by using the relative refractive index $N_R = N^{II}/N^{I}$. Film prisms of this type can be used to analyze the frequency spectrum of a waveguide light beam in some particular mode m, or else for a spatial separation of light of different modes but of one frequency. Thin-film lenses for surface waves were obtained in [20] by shaping the boundary of the region in which the film thickness was changed. The focal lengths of the obtained lenses reached 2 mm. In [21], a rectangular profiled layer of cerium oxide (CeO_2) with thickness 0.08 μ in the center was positive on a film

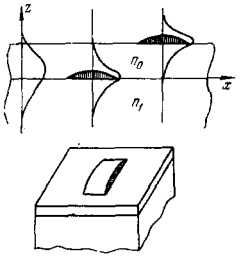

FIG. 5

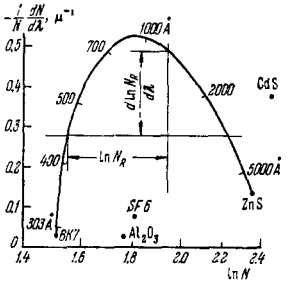

FIG. 6

of glass with $n_0 = 1.64$. The profiling of the layer was carried out during the course of the evaporation of CeO_2 through a rectangular mask located at a distance 1 cm below the substrate. The sputtered section of the film acted like a lens of focal length 12 mm.

An important role in the applications referred to above is played by the dispersion of the refractive index. In thin-film optics, this dispersion can be varied in a wide range by choosing the waveguide parameters, particularly the film thickness h. The dispersion of the relative refractive index can be expressed in the form

$$\frac{d\ln N_R}{d\lambda} = \frac{d\ln N^{II}}{d\lambda} - \frac{d\ln N^{I}}{d\lambda}.$$

If the dispersion (in the case of a ZnS film on VK7 glass, H_I mode, λ = 6328 Å [20]) is plotted against the logarithm of the effective refractive index ($\ln N_R = \ln N^{II} - \ln N^{I}$), we obtain the curve shown in Fig. 6 A thin-film optical waveguide of definite thickness is represented on this plot by a certain point. When the film thickness h is varied, the point moves along the curve joining the points corresponding to the dispersion of the substrate and film material. The film thickness is indicated in Fig. 6 along the curve as a parameter.

It should be noted that the dispersion of the waveguide can be appreciably higher than the dispersion of the material of the waveguide. This property is inherent in the mechanism of waveguide propagation of radiation. If we are interested in particular values of the dispersion and of the relative refractive index of the transition from one film thickness h_I to another h_{II}, then obviously, by suitable choice of the points on the curve of Fig. 6, we can obtain these values simultaneously. In particular, it is possible to have refraction at a boundary between two regions without dispersion, an important factor in the development of achromatic prisms and lenses.

Besides prisms and lenses, diffraction gratings can also be produced in two-dimensional optics. A diffraction grating can be obtained by depositing closely-spaced depressions on the surface of the film or by depositing strips of a dielectric having a low refractive index. The surface-wave propagation constant kn* in such a structure undergoes periodic variations, leading to diffraction effects similar to the scattering of light by a standing acoustic wave in a three-dimensional medium. These phenomena can be used in a large number of thin-film devices such as spectral filters and mode selectors. If material with large absorption is coated on the surface of the film instead of a dielectric, the result is rapid attenuation of the optical surface wave, and this can be used to develop thin-film equivalents of amplitude masks, spatial filters, gratings, and lenses of the type of a Fresnel zone plate. The realiza-

tion of the film diffraction gratings was reported in [21]. One grating was constructed in the form of a series of aluminum strips deposited on the surface of a glass film ($n_0 \approx 1.64$). The width of each strip was 12 μ and the spacing between strips was also 12 μ, the strip length reaching 0.25 mm. When a collimated beam is incident on such a grating, the output beam has a divergence 5° and consists of several beams of higher diffraction orders. Another dielectric grating was produced on the surface of a glass plate with approximate thickness 2 μ, by developing the image of the strips in a thin photoresist layer. The length of the grating along the strips was 1.5 mm. The number of strips reached 40. The strip width and the spacing between strips was 9.6 μ. Propagation of the optical surface wave along such a grating, when the incident beam was approximately parallel to the grating strips, led to the appearance of diffraction orders separated by angles $\theta = \lambda_0/\Lambda$ (λ_0 is the wavelength of the light in the waveguide and Λ is the period of the grating). The measured angular distribution of the diffracted rays in the film (1.24°) was in good agreement with the calculated value of θ.

Thus, all the foregoing shows that film-optics elements (prisms, lenses, gratings), are feasible and can be used in integrated-optics systems.

3. ENTRY AND EXIT OF RADIATION THROUGH THIN-FILM WAVEGUIDES

Dielectric films of thickness on the order of or less than the light wavelength are of greatest interest from the point of view of integrated optics, and in particular for the development of single-mode dielectric waveguides (or waveguides with a limited number of surface waves), for the realization of nonlinear optical transformation in the waveguides, for an effective action of passive optical elements (lenses and prisms) on surface waves in the waveguide plane, etc. The critical film thicknesses corresponding to surface waves of low order lie precisely in the thickness region, and it is here that the minimum effective waveguide thickness and the maximum effective gradient of the refractive index $\partial n_m^*/\partial h$ are reached.

On the other hand, a small film thickness creates definite difficulties when it comes to excitation of surface waves in the film. First, it becomes impossible to effectively introduce radiation through the open end of the thin-film waveguide, since the shaping of the specified distribution of the exciting field at the entrance to such a waveguide becomes a very complicated practical problem (all the more since it becomes additionally aggravated by considerable perturbations of the field on the optically uneven end surface of the film). The methods developed by now for the excitation of a thin-film waveguide through its surface are simpler and are sufficiently effective [6,8,24,30-35].

When it comes to introducing optical energy through the surface of the film, account must be taken of the boundary condition (1.5), according to which a monochromatic wave $\exp[i(\mathbf{k}\cdot\mathbf{r}-\omega t)]$, which excites an m-th surface wave on the side of the second (or first) medium, should have a wave-vector x-component equal to kn_m^*, which exceeds the value $kn_{2(1)}$ of the wave vector in these media. Obviously, the required projection k_x must be possessed by the field penetrating into the second medium (and subsequently into the film) under total

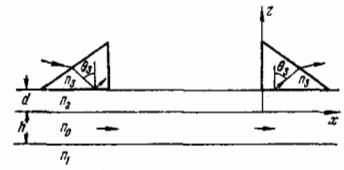

FIG. 7

internal reflection of the light in the optically denser dielectric layer placed over the surface of the film at a certain distance d (Fig. 7). If the refractive index of the layer n_3 exceeds n_m^*, then, using an exciting wave of suitable polarization and selecting the angle of wave incidence on the base of the layer, it is possible to satisfy the condition $n_3 \sin\theta_3 = n_m^*$, i.e., to attain phase synchronism of the exciting wave with the specified surface wave in the direction of its propagation. To introduce a laser beam into a dielectric layer in a direction "synchronized" with a definite mode of the thin-film waveguide, from a surrounding medium that has a lower optical density (e.g., from the second medium), it is necessary to incline the entrance end-face of the layer relative to its base, forming a prism (see Fig. 7). By realizing in this manner the optical tunnel effect in a certain section of the film, it is possible to introduce into it the greater part of the exciting-wave energy. Since the reradiation of the light energy back to the prism becomes stronger as this energy accumulates in the excited surface wave, there should exist an optimal length of the interaction region, corresponding to the most effective introduction of the radiation into the waveguide; this length depends essentially on the gap d between the prism and the film. In addition to the case of introduction of the radiation by the tunnel mechanism [1)], phase synchronism ($k_x = kn_m^*$) of the wave incident on the film and of the surface wave excited by it can be ensured by spatial modulation of the exciting wave with the aid of a phase diffraction grating coated on the surface of the dielectric film. By specifying the period of the diffraction grating and the polarization of the exciting wave, and by choosing the angle of its incidence on the grating, it is easy in principle to obtain the required spatial harmonic $\exp(ikn_m^* x)$ in the distribution of the field of the exciting wave on the surface of the film. In addition to the diffraction and tunnel-effect methods of introducing the optical radiation into the thin-film waveguide, a sufficiently effective method is also the excitation of surface waves through a gradually narrowing edge of the thin film [32]. The ideas of this method and the results of its practical application will be discussed at the end of this chapter.

The optical tunnel effect is frequently used not only for the introduction but also for the extraction of the radiation from the thin dielectric film, as shown in the right-hand side of Fig. 7. The exponentially decreasing field of the surface wave, after reaching the base of the film, penetrates partially into it and goes into the interior in a direction that follows from the boundary condition

$$n_3 \sin\theta_3 = n_m^* \qquad (n_3 > n_m^*). \tag{3.1}$$

The calculation of the damping of the surface wave as it propagates in the waveguide section adjacent to the base of the prism is perfectly analogous to the problem considered in Chap. 1 in the construction of the theory of the thin-film waveguide. In particular, it is easy to verify that the wave field in the additional layer of the

dielectric (j = 3) and in the first three layers is described by the same formula (1.4) as before. For the case when the light is radiated from the surface of the waveguide into the prism, it is necessary to put $C_3^- = 0$. From the continuity of the tangential components of the field on the flat base of the prism (z = d) we can obtain the amplitude ratios C_3^+/C_2^+ and

$$\frac{C_2^-}{C_2^+} = -\exp\left(-i\delta_{23} - 2kd\sqrt{n^{*2} - n_2^2}\right). \tag{3.2}$$

The phase shift δ_{23} is calculated from formula (1.10) in which the subscript 0 is replaced by 3. From the boundary conditions on the upper surface of the film (z = 0) we can determine C_2^+/C_0^+ and

$$\frac{C_0^-}{C_0^+} = e^{-i\tilde{\delta}_{02}}, \quad \operatorname{tg}\frac{\tilde{\delta}_{02}}{2} = \frac{C_2^+ - C_2^-}{C_2^+ + C_2^-}\operatorname{tg}\frac{\delta_{02}}{2}. \tag{3.3}$$

In the absence of a prism ($C_2^- = 0$), the last ratio goes over into the ratio (1.9). As to (1.11), which follows from the boundary conditions on the interface between the film and the first medium, it obviously remains unchanged. Combining (1.11) and (3.3), we obtain the following dispersion equation:

$$2kh\sqrt{n_0^2 - n^{*2}} - \delta_{01}(n^*; n_0, n_1) - \tilde{\delta}_{02}(n^*; n_0, n_2, n_3, kd) = 2\pi(m-1). \tag{3.4}$$

In the weak-coupling case, which is usually realized in practice, i.e., when the distance from the prism to the film is such that

$$\exp\left(-2kd\sqrt{n^{*2} - n_2^2}\right) \ll 1 \tag{3.5}$$

and $|C_2^-/C_2^+| \ll 1$ in accord with (3.2), we get from (3.3)

$$\tilde{\delta}_{02} - \delta_{02} \approx -2\frac{C_2^-}{C_2^+}\sin\delta_{02}. \tag{3.6}$$

Taking now the small deviation of (3.4) from the dispersion equation (1.12) into account, we can easily calculate, by the small-perturbation method, the effective refractive index for a surface wave that is gradually radiated from a thin-film waveguide into a prism:

$$\begin{gathered}\tilde{n}_m^* = n_m^* + \delta n_m^*, \\ \delta n_m^* = \delta n_m' + i\delta n_m'' = -\frac{\sqrt{n_0^2 - n_m^{*2}}}{n_m^* k h^*}\exp\left(-2kd\sqrt{n_m^{*2} - n_2^2}\right)\sin\delta_{02}\cdot e^{-i\delta_{23}},\end{gathered} \tag{3.7}$$

where the effective waveguide thickness h* defined in (1.22a), together with the phase shifts $\delta_{02(23)}$, is calculated at the value $n^* = n_m^*$. Thus, the distribution of the field along the waveguide takes the form $\exp(ikn_m^* x) = \exp(-\alpha x)\exp(i\beta x)$, where the damping coefficient is $\alpha = k\delta n_m''$ and the propagation constant is $\beta = k(n_m^* + \delta n_m')$.

In the case of smooth variations of the gap and of the film thickness along the waveguide, and more accurately speaking in the WKB approximation

$$\frac{d\ln d(x)}{d(kx)} \ll 1, \quad \frac{d\ln h(x)}{d(kx)} \ll 1 \tag{3.8}$$

the solution of the problem of tunnel extraction of optical radiation from a thin-film waveguide retains the form (3.7), but it is necessary to take into account the fact that in this case it is not only the quantities d and h, but also the effective refractive index $n_m^*(kh)$ depends implicitly on x, in accordance with the dispersion equation (1.13). There is no practical advantage in larger changes of the coupling condition along the waveguide, with increments $\Delta d \sim d$ and $\Delta h \sim h$ over distances on the order of the wavelength, since they lead to an appreciable scattering of the optical energy as a result of partial reflection of the surface wave, its transformation into other surface waves, and intensive radiation in directions that differ significantly from the direction indicated in (3.1). In the presence of weak coupling between the film and the prism, the dimension of the light beam radiated from the surface is $\Delta x \gtrsim 1/\alpha$ and greatly exceeds the wavelength: $kn_m^* \Delta x \gtrsim n_m^*/\delta n_m'' \gg 1$. Under these conditions, by choosing sufficiently smooth profiles of d(x) and h(x), it is possible to obtain in the outgoing light beam a field distribution with a profile specified beforehand in accordance with some additional considerations. We note by way of a preliminary that at sufficiently small path sections dx, as in the homogeneous case (relative to the x axis) d = const, h = const, the surface wave acquires an increment

$$d\ln X(x) = ik\tilde{n}_m^*(kh, kd)\,dx. \tag{3.9}$$

By specifying the field distribution X(x) in the form $\sqrt{I(x)}\exp[i\varphi(x)]$ and substituting the solution (3.7) in (3.9), we arrive at the following equations that determine the profile of the film h(x) and the profile of the gap d(x):

$$\frac{d\varphi(x)}{dx} = k[n_m^*(kh) + \delta n_m'(kd, kh)] \approx kn_m^*(kh), \tag{3.10}$$

$$\frac{1}{2I(x)}\frac{dI(x)}{dx} = -k\delta n_m''(kd, kh). \tag{3.11}$$

We see from (3.10) that the distribution of the phase of the radiated wave (for example, at the base of the prism) depends mainly on the film profile h(x). In particular, the wave radiated from a film of constant thickness is approximately plane, and weak distortions of its form appear when the gap d(x) between the film and the prism is varied. First, inasmuch as the optical-energy flux $P_x(x)$ carried along the waveguide by the surface wave is proportional to the wave intensity, it is possible to replace I in the left-hand side of the equation by P_x. This flux is attenuated by transfer of energy to the prism, i.e., $-dP_x/dx = dP_3/dx = S_3(x)$, where the latter quantity denotes the power radiated from a unit length of a thin-film waveguide. The light fluxes P_x produced by the surface wave in sections x and x′ of the waveguide are connected by the relation

$$P_x(x) = \int_x^{x'} S_3(\eta)\,d\eta + P_x(x'), \tag{3.12}$$

and when this relation is taken into account Eq. (3.11) takes the form

$$\frac{S_3(x)}{\int_x^{x'} S_3(\eta)\,d\eta + P_x(x')} = 2k\delta n_m''(kd, kh). \tag{3.13}$$

Substituting in (3.13) the expression for $\delta n_m''$ from (3.7) we obtain a formula for the profile d(x) of the gap between the film and the prism:

$$\begin{aligned}2\sqrt{n_m^{*2} - n_2^2}\,kd(x) = \ln\left[2\sqrt{n_0^2 - n_m^{*2}}\sin\delta_{02}(n_m^*)\sin\delta_{23}(n_m^*)/n_m^*\right] \\ + \ln\frac{\int_x^{x'} S_3(\eta)\,d\eta + P_x(x')}{h^*(n_m^*)\,S_3(x)}.\end{aligned} \tag{3.14}$$

So far we have assumed throughout that the time dependence of the field is given by $\exp(-i\omega t)$. However, as shown by the outlined solution, all the results remain in force also for a time dependence $\exp(i\omega t)$. In other words, in view of the reversibility of optical phenomena in time, the description given above for the tunneling extraction of optical radiation from a thin film into a prism can be directly extended to the inverse process of tunneling excitation of a thin-film waveguide. The absence of a wave reflected from the base of the prism indicates that the wave incident on the prism, with a phase distribution $\varphi(x)$ and a power distribution $S_3(x)$,

is completely "infused" in the given m-th mode of the waveguide, if the film thickness h(x) and the gap d(x) vary along the waveguide in accordance with (3.10) and (3.14).

Let us dwell in greater detail on the optimal conditions for the excitation of a thin-film waveguide with the aid of a paraxial light beam. In the case of slight curvature of the phase front of the exciting wave near the base of the prism, the phase distribution on the front is given by

$$\varphi(x) = \varphi(0) + kn_3 \sin\theta_3 \cdot x - \frac{kn_3 \cos^2\theta_3}{2R} x^2, \qquad (3.15)$$

where θ_3 is the angle of incidence of the wave on the base of the prism (i.e., the angle between the beam axis and the z axis) and R is the radius of curvature of the phase front, which assumes positive values in the case of a diverging incident beam and negative values in the opposite case ($x/|R| \ll 1$ inside the beam). According to condition (3.10) for the phase synchronism between the exciting wave and the m-th surface wave, the effective refractive index should vary along the waveguide in the following fashion:

$$n_m^*(kh) = n_3 \sin\theta_3 - n_3 \cos^2\theta_3 \frac{x}{R} - \delta n_m'(kd, kh).$$

Since the last two terms are small, the effective refractive index is $n_m^* \approx n_3 \sin\theta_3 \equiv N$, and the film thickness h_m determined by the dispersion equation (1.13) remains approximately constant: $h(n_m^*) \approx h(N) \equiv H_m$. Taking this into account in the term $\delta n_m'$, we obtain from (1.13) by the small-perturbation method the optimal film profile $h_m(x)$:

$$h_m(x) = H_m - \frac{Nh^*(N)}{n_0^2 - N^2}\left[\delta n_m'(kd, kH_m) + \frac{n_3^2 - N^2}{n_3}\frac{x}{R}\right], \qquad (3.16)$$

where the gap profile d(x) is so far arbitrary. The optimal profile d(x) of the gap between the film and the prism is calculated with sufficient accuracy by formula (3.14) at $n_m^* = N$. Thus, only the last term depends on x. We see that the optimal profile d(x) is determined completely by the distribution of the exciting beam power $S_3(x)$ at the base of the prism.

In the case of a paraxial beam with Gaussian field distribution over the cross section ($|v_3(\tilde{x}')| \sim \exp(-x'^2 w_0^2)$), which is of practical importance, the relative distribution of the power at the prism base is given by

$$S_3(x) = \exp(-2x^2/w^2),$$

where $w = w_0/\cos\theta_3 = n_3 w_0/\sqrt{n_3^2 - N^2}$. Substituting this distribution in (3.14) and putting $x' = \infty$ and $P_x(x') = 0$, we obtain first the optimal size of the gap at the center of the exciting beam (x = 0)

$$2k\sqrt{N^2 - n_z^2}\, d(0) = \ln\sqrt{\frac{\pi}{2}}\frac{\sqrt{n_3^2 - N^2}\sin\delta_{02}(N)\sin\delta_{23}(N)}{N}\frac{w}{h^*(N)}.$$

On going to another point x, the optimal gap size changes as follows:

$$2k\sqrt{N^2 - n_z^2}\,[d(x) - d(0)] = \ln\frac{1 - \operatorname{erf}(\sqrt{2}\,x/w)}{\exp(-2x^2/w^2)}; \qquad (3.17)$$

Here erf z is the error function

$$\operatorname{erf} z = \frac{2}{\sqrt{\pi}}\int_0^z e^{-\zeta^2} d\zeta.$$

The gap profile corresponding to (3.17) is shown in Fig. 8 [2)]. Since 99% of the power of a Gaussian beam is contained in the interval $-1.5 < x/w < 1.5$ we can, confining

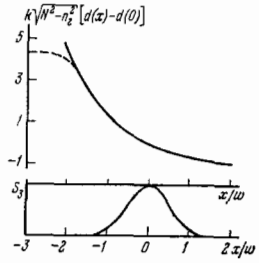

FIG. 8

ourselves to this efficiency of entry of the radiation into the film, maintain a constant gap (shown dashed in Fig. 8) in a waveguide section $x < -1.5w$ or break the coupling between the waveguide and the prism, by placing the left edge of the prism at the point $x \approx -1.5w$.

The determination of the optimal film and gap profiles that ensure total entry of a given light beam into a definite mode of a thin-film waveguide is a complicated practical problem. This raises the question of the effectiveness of tunnel excitation of a waveguide in those cases when the distribution $v_3(x)$ of the exciting field at the base of the prism differs significantly from the field phase and intensity distributions $\varphi(x)$ and $S_3(x)$ that follow from (3.10) and (3.14) for specified profiles h(x) and d(x). A relatively simple formula for the estimate of the input effectiveness as a ratio of the power of the excited surface wave to the total power of the incident wave can be derived under sufficiently general assumptions [31]:

$$\eta = \frac{\left|\int_{x''}^{x'} v_3(x)\sqrt{S_3(x)}\, e^{-i\varphi(x)}\, dx\right|^2}{\int_{x''}^{\infty} S_3(x)\, dx \int_{-\infty}^{\infty} |v_3(x)|^2\, dx}, \qquad (3.18)$$

where the integration is carried out over the waveguide section $x'' < x < x'$, within the limits of which the radiation is admitted. This formula is valid not only for tunnel excitation of a waveguide (under the condition of weak or strong coupling), but also when the waveguide is excited by other methods (for example, diffraction entry of radiation into a thin film).

We now estimate the effectiveness of tunnel entry of certain beams into a film of constant thickness at a constant value of the gap between the film and the prism, in a section $0 < x < \infty$ within which a weak coupling of the incident beam with the exciting waveguide is maintained. In this case, the optimal field distribution in the incident light beam corresponds to

$$\varphi(x) = \beta_m x, \quad S_3(x) = \exp(-2\alpha_m x), \quad 0 < x < \infty,$$

where β_m and α_m are constants: $\beta_m = k(n_m^* + \delta n_m')$ and $\alpha_m = k\delta n_m''$; $\delta n_m'$ and $\delta n_m''$ are defined in (3.7). Let us assume further that the waves incident on the base of the prism have a plane phase front and are synchronized in phase with the m-th mode of the waveguide: $kn_3 \sin\theta_3 = \beta_m$. Then, if the amplitude of the exciting field is uniformly distributed over the section $0 < x < l$, namely

$$v_3(x) = A_3 e^{i\beta_m x}, \quad A_3 = \begin{cases} 1 & (0 < x < l), \\ 0 & (x < 0,\ x > l), \end{cases}$$

the entry efficiency is

$$\eta = \frac{\left(\int_0^l e^{-\alpha_m x}\, dx\right)^2}{l\int_0^{\infty} e^{-2\alpha_m x}\, dx} = \frac{2}{\alpha_m l}(1 - e^{-\alpha_m l})^2.$$

Excitation of the m-th surface wave by a homogeneous beam is the most effective under the condition $\alpha_m l$

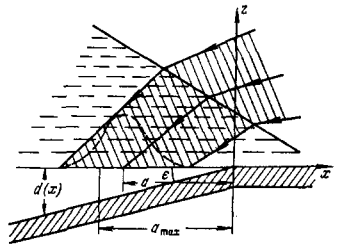

FIG. 9

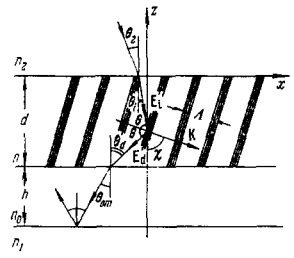

FIG. 10

$= 1.25$; $\eta_{max} = 81\%$ [11]. In the case of an exciting beam with a Gaussian field-amplitude distribution at the base of the prism, namely

$$v_3(x) = \exp\left[i\beta_m x - \frac{(x-a)^2}{w^2}\right],$$

the tunnel-input efficiency is given by

$$\eta = \sqrt{\frac{\pi}{2}}\alpha_m w \exp\left(\frac{\alpha_m^2 w^2}{2} - 2\alpha_m a\right)\left[1 + \operatorname{erf}\left(\frac{a}{w} - \frac{\alpha_m w}{2}\right)\right]^2.$$

The latter reaches its maximum value 0.801 under the conditions

$$1{,}462\alpha_m w \approx 1 \text{ and } 2\alpha_m a = 1,$$

which determine the optimal half-width w of a Gaussian beam and the optimal shift a of its center relative to the left-hand edge of the prism [31].

The experimentally attained radiation-entry efficiencies at a constant gap between the prism and the film do not exceed 57% [24].

To estimate the efficiency of the tunneling entry of light beams into a thin film with arbitrary profile h(x) at an arbitrary profile d(x) of the gap between the film and the prism, it is necessary to know the optimal field distribution, corresponding to this more general case, in the exciting beam. Integrating (3.10) and (3.11) and recognizing that $S_3(x) \sim -dI/dx$, we obtain

$$\sqrt{S_3(x)}\, e^{i\varphi(x)} = v_3^{(0)}(x) = \sqrt{\delta n_m''}\exp\left[-k\int^x \delta n_m'\, dx + ik\int^x (n_m^* + \delta n_m')\, dx\right], \tag{3.19}$$

where $\delta n_m'(kd, kh)$ and $\delta n_m''(kd, kh)$ are given by (3.7). We indicate no definite lower limit of integration in (3.17), since the choice of this limit does not influence the relative field distribution. If phase synchronism exists between the incident beam and the excited (m-th) mode of the thin-film waveguide, the phase factors cancel each other in the numerator of (3.18). We recall that to ensure phase synchronism in the case of a paraxial exciting beam the film thickness should vary along the waveguide in accordance with (3.16). We can therefore $h = H_m = \text{const}$ put in $\delta n_m''(kd, kh)$, with sufficient accuracy. Under these limitations, the optimal distribution of the exciting-field amplitude takes the form

$$|v_3^{(0)}(x)| = e^{-\sqrt{n_m^{*2} - n_3^2}\, kd(x)} \exp\left[-D^{-1}\int^x e^{-2\sqrt{n_m^{*2} - n_3^2}\, kd(x)}\, dx\right],$$

where $D = n_m^* h^* / (\sqrt{n_0^2 - n_m^{*2}} \sin\delta_{02} \sin\delta_{23})$. In particular, for a wedge-shaped gap

$$d(x) = -\varepsilon x, \quad x < 0,$$
$$|v_3^{(0)}(x)| = e^{x/b}\exp\left(-\frac{b}{2D}e^{2x/b}\right); \tag{3.20}$$

here

$$b = (k\varepsilon\sqrt{n_m^{*2} - n_3^2})^{-1}.$$

The distribution (3.20) reaches a maximum at a point shifted to the left from the vertex of the wedge by a distance

$$a_{max} = \frac{b}{2}\ln\frac{b}{D}.$$

Approximating the optimal complex-shape profile shown in Fig. 9 by a wedge-like gap, we can in practice admit almost completely into a given waveguide node a light beam with Gaussian field distribution $|v_3(x)| = \exp[-(x+a)^2/w^2]$. [31] To perform calculations within the framework of the weak coupling, it is necessary to assume that the center of the Gaussian beam is shifted relative to the vertex of the wedge by a considerable distance (say, $a/w > 2$). The results of the calculations show that the entry efficiency η reaches a maximum value 0.96 at a beam displacement

$$a = a_{max} - 0{,}271b, \quad \text{or} \quad a = \left(\ln\sqrt{\frac{b}{D}} - 0{,}271\right)b,$$

and at a beam half-width

$$w = 1{,}128b.$$

The experimentally obtained [31] excitation efficiency $\eta \approx 0.88$ is in good agreement with the theoretical value (allowing for the violation of the weak-coupling conditions and other experimental imperfections).

Besides the tunnel entry of radiation into a thin-film waveguide, a rather effective method is excitation of surface waves with the aid of a phase diffraction grating deposited on the surface of the waveguide film. In experimental entry devices one uses both plane and three-dimensional diffraction gratings [33-35]. The latter have the advantage that they ensure, at a suitable thickness and periodic structure, a deep spatial modulation of the incident wave and a predominant conversion of this wave into a diffractive wave of definite order. Three-dimensional sinusoidal gratings are prepared by holographic methods. In particular, when an interference pattern is registered in gelatin sensitized with ammonium bichromate [37,38], lithium niobate [39], and photopolymer materials [40], periodic changes take place in the refractive index (phase gratings). To the contrary, in photochromatic media and ordinary emulsions, amplitude gratings are produced, due to periodic oscillations of the absorption coefficient. A detailed theoretical analysis of three-dimensional sinusoidal gratings, on the basis of the theory of coupled waves, is given in [36].

In accord with this reference, we assume that the refractive index of the medium in a flat inhomogeneous layer of thickness d (Fig. 10) and the absorption coefficient vary harmonically in a direction lying in the (x, z) plane and making an angle χ with the z axis:

$$\tilde{n} = n + \delta n\cos\mathbf{Kr},\ n = n' - in'' = \text{const},\ \delta n = \delta n' - i\delta n'' = \text{const}. \tag{3.21}$$

Here **r** is the radius vector of the point (x, y, z), **K** is

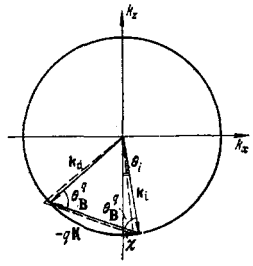

FIG. 11

the vector of the diffraction grating $(2\pi/\Lambda)(\sin\chi, 0, -\cos\chi)$, and Λ is the period of the grating. Since in practice the oscillations of the refractive index and the absorption are small, we can put

$$|\delta n| \ll n', \; n'' \ll n'. \tag{3.22}$$

In the weakly-inhomogeneous layer considered by us, the propagation of a plane monochromatic wave incident on the grating at an angle θ_i and polarized perpendicular to the incidence plane (x, z), i.e., propagation of a type-H mode, is described by the scalar equation

$$\Delta E + \left(\frac{\omega}{c}\tilde{n}\right)^2 E = 0, \tag{3.23}$$

where $E = E_y(x, z)e^{i\omega t}$ and $\tilde{n}^2 \approx (n'^2 - 2in'n'') + n'\delta n(e^{i\mathbf{Kr}} + e^{-i\mathbf{Kr}})$. It is seen from this equation that when a plane wave $\exp[-i\mathbf{k}_i\cdot\mathbf{r}]$ passes through the grating, besides being partially absorbed, it is converted into a wave of the type $\exp[-i\mathbf{r}\cdot(\mathbf{k}_i \pm \mathbf{K})]$, which in turn generates diffraction waves of higher order, $\exp[-i\mathbf{r}\cdot(\mathbf{k}_i \pm 2\mathbf{K})]$, etc. If the wave $\exp[-i\mathbf{k}_i\cdot\mathbf{r}]$ is incident on homogeneous layers of the grating at an angle θ_B^q, satisfying the Bragg condition

$$2kn'\cos\theta_{iB}^{q} = qK \qquad (q = 1, 2, 3, \ldots),$$

then, as can be easily seen from Fig. 11, the q-th order diffraction wave of $\exp[-i\mathbf{r}\cdot(\mathbf{k}_i - q\mathbf{K})]$ is also scattered at the same angle from these layers. In the particular case $q = 1$, which is considered in [36], in view of the Bragg scattering of the incident wave E_i into a diffraction wave of first order ($E_d \sim \exp[-i\mathbf{k}_d\cdot\mathbf{r}]$, $\mathbf{k}_d = \mathbf{k}_i - \mathbf{K}$), a strong coupling is established between these waves (if the grating is thick enough), and diffracted waves of higher orders can therefore be neglected in first-order approximation. Thus, the optical field inside the inhomogeneous layer can be represented in the form of a superposition of two waves

$$\begin{aligned} E_i(x, z) &= A_i(z)\exp(-i\mathbf{k}_i\mathbf{r}), \\ E_d(x, z) &= A_d(z)\exp(-i\mathbf{k}_d\mathbf{r}), \end{aligned} \tag{3.24}$$

where the wave vectors are $\mathbf{k}_i = kn'(\sin\theta_i, 0, -\cos\theta_i)$ and $\mathbf{k}_d = kn'(\sin\theta_i - (k/kn')\sin\chi, 0, -\cos\theta_i + (K/kn')\cos\chi)$, while the complex amplitudes $A_i(z)$ and $A_d(z)$ vary slowly along the z axis as a result of absorption and mutual conversion of these waves into each other. In connection with the use of a three-dimensional diffraction grating for the entry of optical radiation into a thin-film waveguide, it is appropriate to note here that the Bragg condition used above is, strictly speaking, not compatible with the requirement that phase synchronism exist between the diffraction wave E_d and the m-th waveguide mode exciting it. Thus, by virtue of the first condition, the wave vector k_d is equal to kn'. To satisfy the second condition, on the other hand, it is necessary that the wave vector of the diffraction wave exceed kn_m^*, and all the more kn'. In view of this we shall assume that the vector $\mathbf{k}_d$ goes outside the limits of the circle of radius kn' drawn in Fig. 11 with the origin of the wave vector $\mathbf{k}_i$ as the center, and that the Bragg condition is satisfied only approximately:

$$\theta \equiv \chi - \theta_i = \theta_{Bl}^{l} + \delta\theta, \quad \delta\theta \ll \theta_{Bl}^{l}, \tag{3.25}$$

$$2kn'\cos\theta_{B}^{l} = K. \tag{3.26}$$

Substituting in the wave equation (3.23) the field E in the form of a sum of waves (3.24) and equating the zero the coefficients of the independent factors $\exp(-i\mathbf{k}_i\cdot\mathbf{r})$ and $\exp(-i\mathbf{k}_d\cdot\mathbf{r})$, we obtain the following equations for the amplitudes of the incident and diffracted wave:

$$\begin{aligned} \frac{i}{2kn'}\frac{d^2A_i}{dz^2} - c_i\frac{dA_i}{dz} + \alpha A_i &= -i\varkappa_H A_d, \\ \frac{i}{2kn'}\frac{d^2A_d}{dz^2} - c_d\frac{dA_d}{dz} + (\alpha + i\tau)A_d &= -i\varkappa_H A_i, \end{aligned} \tag{3.27}$$

where

$$\begin{aligned} c_i &= \cos\theta_i, \qquad c_d = \cos\theta_i - \frac{K}{kn'}\cos\chi, \qquad \alpha = kn'', \\ \varkappa_H &= \frac{1}{2}k\delta n, \qquad \tau = K\left(\cos\theta - \frac{K}{2kn'}\right) \approx -K\sin\theta_{B}^{l}\cdot\delta\theta. \end{aligned} \tag{3.28}$$

We can analogously derive from the wave equation $\nabla^2 E$ $\nabla(\nabla E) + (\omega\tilde{n}/c)^2 E = 0$ approximate equations for the amplitudes of the electric field A_i and A_d in the case when the incident wave, and consequently also the diffracted wave, is polarized in the incidence plane x, z ($H_i = H_i, y$, $H_d = H_d, y$). To go over to these equations from (3.27), it suffices to replace κ_H by $\kappa_E = -(1/2)k\delta n\cos 2(\theta_i - \chi)$.[36] We confine ourselves henceforth to H waves. It is easily seen from (3.27) that under the conditions (3.22) and (3.25) the amplitudes A_i and A_d undergo negligible changes over distances on the order of the wavelength, and terms with second derivatives in these equations can be omitted. In this case, the general solution of (3.27) contains two arbitrary constants $r_{1,2}$, which are determined from the initial conditions on the boundary surfaces of the grating $z = 0$ and $z = -d$. In particular, the amplitude of the incident wave at the entry to the grating, i.e., $A_i(0)$, can be conveniently set equal to unity. If the diffraction grating operates in transmission (the parameter $c \equiv k_{i,z}/k_{d,z} = c_i/c_d > 0$), then the wave E_d develops in the direction from the upper surface of the grating ($z = 0$) to the lower one ($z = -d$), having a zero amplitude at $z = 0$. The diffracted wave at the exit from such a grating ($z = -d$) is characterized by the amplitude

$$A_d(-d) = -i\sqrt{c}\exp(-\alpha d/c_i)\,e^{\psi}\sin\sqrt{\nu^2 - \psi^2}/\sqrt{1 - (\psi^2/\nu^2)}, \tag{3.29}$$

where

$$\nu = \varkappa_H d/|c_i c_d|^{1/2} \qquad \psi = \frac{d}{2}\left(\frac{\alpha}{c_i} - \frac{\alpha}{c_d} - i\frac{\tau}{c_d}\right). \tag{3.30}$$

In the case of a reflecting grating (parameter $c < 0$), the wave E_d develops in the opposite direction (along the z axis). Accordingly, the amplitude A_d at $z = -d$ is equal to zero, and at the exit ($z = 0$) the amplitude of the diffraction wave is equal to

$$A_d(0) = \sqrt{c}\,\mathrm{sh}(\nu\,\mathrm{ch}\,a)/\mathrm{ch}(a + \nu\,\mathrm{ch}\,a); \tag{3.31}$$

$\sinh a = \psi/\nu$, where ν and ψ are defined in (3.30).

We shall be primarily interested in the efficiency of conversion of the incident wave E_i into the diffracted wave E_d; this efficiency is characterized by the ratio of the light flux produced by the wave E_d at the exit from the diffraction grating to the optical-energy flux carried by the wave E_i through the entrance surface of the grating $z = 0$:

$$\eta = \left|\frac{k_{d,z}}{k_{i,z}}\right|\frac{|A_d|^2}{|A_i(0)|^2} = \frac{|A_d|^2}{|c|}, \tag{3.32}$$

where the amplitude A_d is described by (3.29) if $c>0$ and by (3.31) if $c<0$. At an incidence angle θ_i corresponding to Bragg diffraction of the incident wave by a three-dimensional grating, ($\theta_i \approx \theta_i^B = \chi - \theta_B^1$), we have

$$c \approx -\cos\theta_i^{BB}/\cos(\theta_i^{BB} - 2\chi).$$

In the absence of absorption (n'', $\delta n'' = 0$), the diffraction efficiency of the transmitting phase grating takes the form

$$\eta = (\sin\sqrt{\nu^2+\xi^2})^2/[1+(\xi^2/\nu^2)],$$

where $\nu = \delta n' kd/2\sqrt{|c_i c_d|}$ and $\xi = \tau d/2|c_d|$. At incidence angles θ_i close to the Bragg angle θ_i^B for the given wavelength of the incident light (see (3.26) with $\theta_B^1 = \chi - \theta_i^B$), we have

$$\xi \approx \tfrac{1}{2} Kd\,\delta\theta_i \sin(\chi - \theta_i^B)/|\cos(\theta_i^B - 2\chi)|,$$

$$\delta\theta_i = \theta_i - \theta_i^B \ll \theta_i^B.$$

On the other hand, if the incidence angle θ_i is specified and we consider small deviations of the wavelength λ from $\lambda_B = 2\Lambda n' \cos(\chi - \theta_i)$, then it is convenient to represent the parameter ξ in the form

$$\xi \approx -K^2 d\,\delta\lambda/8\pi n' \,|\cos(\theta_i - 2\chi)|,$$
$$\delta\lambda = \lambda - \lambda_B \ll \lambda_B.$$

Thus, the dependence of η on ξ, shown in Fig. 12 for three values of the second parameter ν, describes the angular and spectral characteristics of a transmitting diffraction grating. The maximum efficiency for the conversion of the incident wave E_i into a diffracted wave E_d is obtained in the case of Bragg diffraction ($\xi = 0$). For $\nu = \pi/2$ we have $\eta_{max} = 1$ and for $\nu = \pi/4$ and $3\pi/4$ we have $\eta_{max} = 0.5$. The half-width of the maximum is $\Delta\xi \approx 1.5$.

In the case of a reflecting non-absorbing phase grating, the diffraction efficiency is

$$\eta = \{1 + [(1 - \xi^2/\nu^2)/(\sh\sqrt{\nu^2 - \xi^2})^2]\}^{-1}$$

and its dependence on the parameter ξ is entirely different. As seen from Fig. 13, with increasing parameter ν the half-width $\Delta\xi$ of the maximum increases strongly, this being a factor contributing to the increase in the efficiency of the diffraction entry of the radiation into the thin-film waveguide, inasmuch as to ensure phase synchronism between the diffracted wave and the surface wave excited by it it is always necessary to deviate from the conditions of Bragg diffraction ($\xi \neq 0$). With increasing ν, the maxima of the diffraction efficiency become higher: $\eta_{max} = 0.43$, 0.84, and 0.96 for $\nu = \pi/4$, $\pi/2$, and $3\pi/4$, respectively.

The presence of absorption in three-dimensional phase gratings ($n'' \neq 0$, $\delta n'' = 0$) not only lowers the absolute value of the diffraction effectiveness, but also influences, generally speaking, greatly their spectral-angular characteristics [36]. The influence of absorption on the absolute value of diffraction efficiencies of different phase gratings is illustrated in the cited reference in Figs. 8, 14, and 15. We note also that amplitude three-dimensional gratings ($\delta n' = 0$, $\delta n'' \neq 0$) are considered in detail in [36]. In particular, it is shown that the efficiency of conversion of the incident wave into the diffracted wave is largest ($\approx 7.2\%$) in the case of a reflecting amplitude grating with horizontally arranged homogeneous layers ($\chi = 0$, $c = -1$) at a Bragg angle of incidence on the grating ($\xi = 0$), at maximum modulation of the absorption coefficient in the grating ($k\delta n'' = kn''$

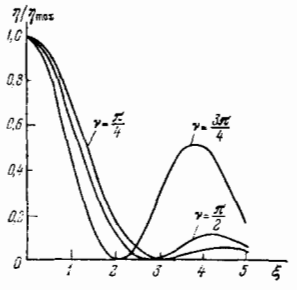

FIG. 12

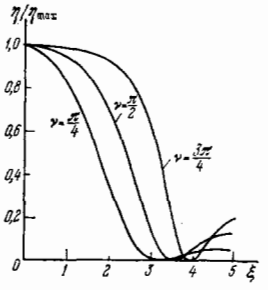

FIG. 13

$= \alpha$), and sufficient thickness of the grating ($D = \alpha d \cos\theta_i^B > 2$). Naturally, all the results presented above are valid for three-dimensional diffraction gratings of sufficient thickness or, more accurately speaking, under the condition

$$K^2 d/kn' \gg 1,$$

which is well satisfied in practice [36]. An entry device making use of a three-dimensional diffraction grating was realized experimentally in [34]. To obtain a dielectric diffraction grating, gelatin sensitized with ammonium bichromate was used; the technology of preparation and development of the gelatin is described in detail in [41]. A gelatin layer of thickness $d = 4\ \mu$ was coated on a waveguide film by immersing the substrate with the film in the gelatin solution and then drawing it out of the solution at a constant rate. The waveguide film, made of glass, had a thickness $h = 0.3\ \mu$ and a refractive index n_0 equal to 1.62. The input device was designed for a wavelength $\lambda = 6328$ Å and for a light incidence angle on the grating θ_i close to zero. The homogeneous layers in the diffraction grating of such an exciting device should be inclined at an angle $\chi = 45°$ and should have a spatial period Λ equal to $0.25\ \mu$. A grating with the indicated dimensions was obtained by exposing sensitized gelatin to He-Cd laser radiation with $\lambda' = 4416$ Å. Two coherent light beams from the cadmium laser, incident on the gelatin at suitable angles, produced a three-dimensional interference pattern. Further processing of the gelatin by a method similar to that used in holography has made it possible to obtain a three-dimensional diffraction grating measuring 5×5 mm. The light entered the film through the grating operating either in the transmission region or in the reflection region, but the best results were obtained when a reflecting diffracting grating was used (i.e., when the light was incident on the grating from the side of the substrate). In the experiment, the exciting laser beam has a Gaussian field distribution and was incident on the edge of the grating. To optimize the entry of the light, the parameter $2w_0$ of the beam at the focus and the distance from the focus to the grating were varied. For the best of the gratings, the most effective input was with the aid of a diverging beam of diameter $2w_0 = 0.3$ mm with the focus 16 cm away from the grating (the beam diameter on the grating amounted in this case to $2w = 0.6$ mm). The optimal dimensions of the region within which the radiation was admitted were of the same magnitude (≈ 0.6 mm). The study of the angular dependence of the transmission of the grating when an H wave was excited in the film (under optimal conditions) has shown that the insertion efficiency reaches a maximum when the angle of incidence of light on the substrate is $\theta = 3°$, and decreases to half this value when the angle is changed by an amount $\Delta\theta$

~0.1°. The Bragg condition was satisfied near the angle of incidence $\theta = 6°$, and the width of the "Bragg resonance" was $2\delta\theta = 3°$. Measurement of the reflection and transmission of the grating has made it possible to estimate the efficiency of entry of the optical energy into the film. It amounted to 71°. The efficiency of excitation of an E wave in the film with the aid of such a grating did not exceed 15%.

In addition to a three-dimensional diffraction grating, the light can be fed to the film also through a flat diffraction grating. The first exciting device with a flat diffraction grating was proposed and realized in [33]. Just as the three-dimensional grating, the flat diffraction grating is deposited directly on the waveguide film. The laser beam incident on the sinusoidal phase grating with period Λ and phase-modulation depth $\Delta\Phi$ at an angle θ_i produces on the film surface a polarization wave with a phase factor in the form

$$\exp\left[i\left(\Delta\Phi\sin\frac{2\pi x}{\Lambda}+\frac{2\pi x}{\lambda}\sin\theta_i\right)\right].$$

This polarization wave can be represented in the form of a superposition of spatial harmonics

$$\exp\left[i\left(\frac{2\pi x}{\Lambda}q+\frac{2\pi x}{\lambda}\sin\theta_i\right)\right],$$

$q = 0, 1, 2, 3, \ldots$ The polarization wave will excite in the film the m-th surface wave $\exp(ikn_m^* x)$ if one of the spatial harmonics of the polarization wave is reconciled in phase with the surface wave:

$$n_m^* = \sin\theta_i + \frac{q\lambda}{\Lambda}. \qquad (3.33)$$

This condition determines the connection between the parameters of the grating, the film, and the incidence angle θ_i.

To excite a surface wave in a glass film of thickness $h = 0.76\ \mu$ and with $n_0 = 1.73$, deposited on a glass substrate with $n_1 = 1.52$, use was made of a flat diffraction grating of a photoresist with a period $\Lambda = 0.665\ \mu$. An entry efficiency $\approx 40\%$ was reached in this experiment. The surface waves excited in the film were identified with the aid of formula (3.33) on the basis of calculated dispersion curves and measured values of the incidence angle θ_i.

In another study [35], the phase diffraction grating for the entry of the radiation was produced directly in the waveguide film as shown in Fig. 14. The waveguide film was made of photoresist, and the phase diffraction grating was formed in it, just as in [33], by using an argon laser with $\Lambda = 4880$ Å. The radiation-entry efficiency reached ≈50%.

In concluding this chapter, let us dwell in greater detail on the insertion and extraction of the radiation through a tapering edge of the waveguide film. The dimensions l of the tapering region will be assumed to be much smaller than the wavelength λ. As indicated above, the effective refractive index $n_m^* = n_0 \sin\theta_{0m}$ for the m-th wave in the film depends on the film thickness and decreases monotonically in the region of the tapering-down edge, reaching at a certain point x_{cr} (as the film thickness approaches the critical thickness h_m^{min}) the value n_1 of the diffractive index of the substrate. With further propagation in the film, the angle of incidence θ_{0m} of the wave on its walls decreases such an extent that the wave, no longer experiencing total internal reflection from the interface of the film with the first medium (substrate), is partially refracted into

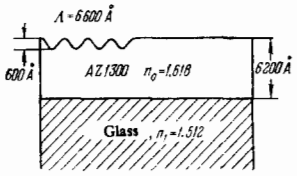

FIG. 14

this medium. It is shown in [32] that in the tapering region of the film the conversion of the surface wave into substrate radiation modes occurs over a distance of several wavelengths ahead of the point x_{cr}. According to calculations, 80% of the light energy radiated into the substrate through the tapering edge of the film should be concentrated in the far zone within an angle 15°. The picture of the field changes little if the slope of the tapering edge ranges from 0.01 to 0.001. An experimental check [32] had demonstrated the feasibility of using the tapering edge of the film for the entry of optical radiation. The exciting unit was constructed by depositing a ZnS film on a polished glass block, part of which was covered during the time of the sputtering by a mask, in order to shape the tapering edge of the film. The taper angle determined by the distance from the mask to the surface of the glass block, was 0.001. The film thickness h, equal to 1420 ± 50 Å, was such as to be able to excite in the film the fundamental surface mode H_1. A laser beam with $\lambda = 6328$ Å and a near-Gaussian distribution was focused through the lateral surface of the glass block on the edge of the film. Owing to the scattering of the light in the ZnS, it was possible to observe the trajectory of the excited surface wave. In this experiment, approximately 25% of the laser-beam energy entered the film, and the remainder of the beam was reflected from the boundary between the film and the glass. A similar exciting unit was constructed for an organic film on a glass substrate, and the entry efficiency reached in this case 40%. To increase the entry efficiency it is necessary to monitor the distribution of the intensity of the incident laser beam, so as to match this distribution to the intensity distribution of the radiation modes.

4. NONLINEAR OPTICAL PHENOMENA

The effective methods developed to date for the excitation of a dielectric waveguide through its surface at a low effective waveguide thickness ($h^* \sim \lambda$) make it possible to obtain light fluxes of high density on sufficiently extended film sections. In addition, an advantage of a thin-film waveguide, from the point of view of nonlinear optics, is that in any of the component dielectric layers, made of an optically nonlinear material, it is possible to satisfy the phase-synchronism condition for the interacting surface waves by having the frequency dispersion of the effective refractive indexes offset by the increments that result when the order (m) or the type (H or E) of the surface wave is changed. These increments can be varied in the experiment by varying the film thicknesses and the refractive indices of the adjacent media. We recall that in bulky nonlinear crystals the phase sychronization of the interacting waves is attained only in the presence of optical anisotropy, when the refractive index of the crystal depends on the polarization in the direction of the light-wave propagation. To the contrary, thin-film waveguides provide a means of using optically isotropic nonlinear media.

Let us consider the parametric interaction of three surface waves in a thin flat film of optically isotropic nonlinear material, placed between two optically linear dielectric layers [48]. Assume that the surface pump wave frequency ω''' and the parametrically excited waves with frequencies ω' and ω'' ($\omega'+\omega''=\omega'''$) propagate in the same direction (along the x axis), and have a Gaussian distribution in the plane of the film (with respect to the y axis), and a distribution corresponding to one of the fundamental modes (H_1 or E_1) of the waveguide in its cross section (along the z axis), i.e., corresponding to its minimal effective thickness. At a sufficient width of the Gaussian beam, one can neglect its diffraction divergence in a thin-film waveguide section of length l, and write the condition of phase synchronism in the simple form

$$\omega' n^*_{1,H}(\omega') + \omega'' n^*_{1,H}(\omega'') = \omega''' n^*_{1,E}(\omega'''). \qquad (4.1)$$

The pump wave is chosen here to be an E wave, and the parametric waves are chosen to be H waves, in view of the fact that $n^*_{1,H}(\omega)$ always exceeds $n^*_{1,E}(\omega)$, and this makes it possible to compensate for the dispersion increment of the latter due to the transition from the frequencies ω' and ω'' to the higher frequency ω'''. In other words, relation (4.1) determines the frequencies of the H_1 waves that are parametrically excited in the given waveguide, in terms of the frequency of the pumping E_1 wave. The effective refractive indices are calculated on the basis of the dispersion equation (1.13) at $m=1$ and $\kappa=0$ or two for the H and E waves, respectively. Figure 15a shows the dependence of the parametric frequencies on the relative film which follows from the phase-synchronism condition (4.1) at a pump wavelength in vacuum $\omega'''=1.06\ \mu$ for a GaAs film ($n_0(\omega''')=3.49$) deposited on a substrate of single-crystal CaF_2 ($n_1(\omega''')=1.43$) and placed in air ($n_2(\omega''')=1$) [48]. If the refractive index of one of the media is varied (using, for example, different liquids as a second medium) and the effective refractive indices are changed by the same token, then the parametric frequency can be tuned in sufficiently wide range at a given pump frequency. Thus, putting $n_2(\omega')=n_2(\omega'')=n_2(\omega''')$ and varying n_2 from one to 1.6, we obtain in a film of relative thickness $h/\lambda'''\approx 0.17$ (or $B=hk_0(\omega''')\approx 3.66$) a tuning of the parametric frequency in the range $\omega'''/2\,(1\mp 0.35)$ (see Fig. 15b). The same figure shows also the tuning curves for other values of the parameter B.

When anisotropic nonlinear media are used in the form of a thin film (or substrate), account must be taken also of the fact that in the case of arbitrary orientation of the principal axes of the crystal relative to the plane of the film and the propagation direction of the surface wave, the electric field of the latter at any point of the waveguide varies with time not only in magnitude but also in direction. Averaging over different orientations of the electric vectors of the surface waves relative to the principal axes of the crystal (and relative to one another) leads to a weakening of the nonlinear interaction of the surface waves. This raises the question of the anisotropic-crystal orientations at which the surface-wave electric-vector direction can be maintained constant in the thin-film waveguide, i.e., at which H waves can be realized in the medium: $\mathbf{E}=(0, E_y, 0)$, or at least the electric vector of the surface wave can be contained in a definite plane, i.e., E modes can be realized: $\mathbf{E}=(E_x, 0, E_z)$. The possibilities for the case of a uniaxial crystal are analyzed in [49]. We assume

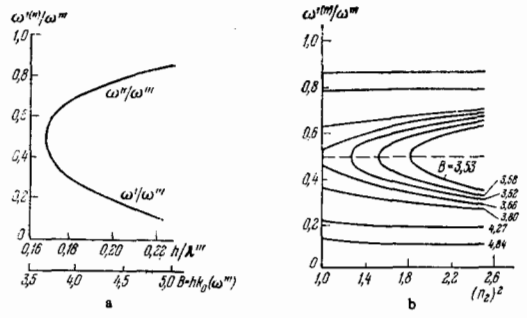

FIG. 15

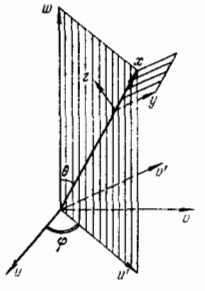

FIG. 16

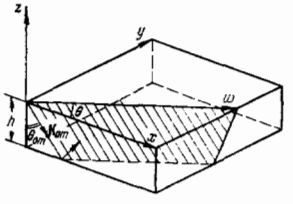

FIG. 17

in accord with that reference that only the film is made of anisotropic material, and the adjacent media are optically isotropic (a uniaxial crystal can also be used either as a first medium or as the second medium). It is easily seen from Fig. 16 that when the crystal optical axis w and the direction of propagation of the surface wave (the x axis) lie in a plane perpendicular to the (x, y) plane of the film, the H wave is the ordinary wave in the crystal and the E wave is the extraordinary wave. It is perfectly understandable that with such a mutual orientation of the optical axis of the crystal and of the direction of the surface wave, the H and E waves propagate in the thin-film waveguide independently, without being transformed into each other. In [49] the results are considered a case in which the crystal optical axis lies in the film plane (Fig. 17). The remark made by the author concerning this case namely that the H and E waves are maintained approximately under conditions of weak birefringence in sufficiently small sections of the waveguide, remains, of course, in force also for an arbitrary orientation of the optical crystal axis in the thin-film waveguide.

Proceeding now to consideration of parametric interaction of three surface waves in an anisotropic waveguide, we confine ourselves to the first case represented in Fig. 16. We assume that the pump wave with frequency ω''' and the parametrically excited waves with frequencies ω' and ω'' ($\omega'+\omega''=\omega'''$) propagate in one direction (along the x axis) and satisfy the scalar phase-synchronism condition (4.1). In this case the effectiveness of the nonlinear interaction of the surface waves at any point of the film is characterized by the quantity

$$d_{ijk}\overline{E_i(\omega''')}\,E_j(\omega')\,E_k(\omega'') = d_{ijk}\overline{e_i(z,\omega''')}\,e_j(z,\omega')\,e_k(z,\omega''), \qquad (4.2)$$

where d_{ijk} is the quadratic-polarization tensor, and E is the electric field of each of the surface waves. In the presence of weak birefringence of light, the electric field of the extraordinary E waves is described by the formula

$$\mathbf{E}^{(e)} = \mathbf{A}^{(e)}\,e(z)\exp i(kn^*x - \omega t), \qquad (4.3)$$

where e(z) is a real function, $\mathbf{A}^{(e)}=(1+\gamma_2)^{-1/2}(i\gamma, 0, 1)$ is a unit complex vector, $\gamma(z)$ is a real function, and $\mathbf{A}^{(e)}\cdot\mathbf{A}^{(e)}=1$. The electric field of the ordinary H wave can be represented in similar form

$$\mathbf{E}^{(0)} = \mathbf{A}^{(0)}\, e(z) \exp i(kn^*x - \omega t), \qquad (4.4)$$

where $\mathbf{A}^{(0)}=(0, 1, 0)$. We rewrite (4.2) with allowance for (4.3) and (4.4):

$$d_{ijk}\overline{E_i(\omega'')}\, E_j(\omega')\, E_k(\omega'') = C_I e(z, \omega'')\, e(z, \omega')\, e(z, \omega''),$$
$$C_I = d_{ijk}\overline{A_i(\omega'')}\, A_j(\omega')\, A_k(\omega'').$$

It must be emphasized that the coefficient C_I introduced here depends not only on the symmetry properties and orientation of the nonlinear crystal, but also indirectly (via the function $\gamma(z)$ contained in the vector $\mathbf{A}^{(e)}$) also on the coordinate z. The latter circumstance was lost sight of in [49]. It was therefore assumed there that the efficiency of the nonlinear interaction of the surface waves over the entire film cross section, i.e., the quantity

$$\int_0^h d_{ijk}\overline{E_i(\omega'')}\, E_j(\omega')\, E_k(\omega'')\, dz$$

can be reduced to the form

$$C_I \int_0^h e(z, \omega')\, e(z, \omega'')\, e(z, \omega'')\, dz.$$

In fact, the coefficient C_I is independent of γ only in the case of the interaction of three H waves, and consequently this coefficient characterizes the efficiency of the nonlinear interaction over the entire film cross section. In the general case the coefficient C_I determines the nonlinear interaction of surface waves in the vicinity of a certain point, more accurately speaking at all points of a fixed longitudinal plane z = const. The table lists the final formulas for $|C_I|$ from [49], corresponding to different combinations of the interacting surface waves: H–HH, E–HH, and H–EH. We note that the first letter in the indicated combination indicates the type of the pumping wave. Similar formulas were obtained in [49] for parametric interactions with participation of two or three E waves, and are not listed in the table, since these formulas do not take into account that two E waves with different frequencies or of different order correspond to different functions $\gamma(z)$. The coefficients C_I were calculated in [49] for crystals having different symmetry at arbitrary orientation (Θ, φ) in the waveguide film.

The properties of nonlinear optical waveguides can be used to excite radiation at combination frequencies of the initial waves (and also for second-harmonic generation). A theoretical analysis of the production of combination waves in nonlinear thin-film waveguides is presented in [29]. When surface waves of two different frequencies (ω' and ω'') propagate in the film, the nonlinear interaction produces polarization waves that serve as radiation sources at the sum and difference frequencies. The propagation of these waves is characterized by an effective refractive index

$$n_{\pm}^* = \frac{k_x' + k_x''}{\omega' \pm \omega''} c.$$

The quantity $n_{\pm}^*$ depends on the film thickness, on the propagation direction, and on the type of waves of frequency ω' and ω'', and can vary in a wide range. In the particular case when waves of equal frequency propagate in opposite directions, the effective refractive index for the polarization waves at the second-harmonic

Symmetry class	$\lvert C_I\rvert$ for H – HH interaction	$(1/C)\lvert C_I\rvert$ for the interactions E – HH and H – EH (or H – HE)
$\bar{6}2m$	$d_{22}\cos 3\varphi$	$d_{22}\sigma_+ \sin 3\varphi$
$4mm$, 4 / $6mm$, 6	0	$d_{15}\sigma_-$
422 / 622	0	0
$\bar{6}$	$d_{22}\cos 3\varphi + d_{11}\sin 3\varphi$	$(d_{22}\sin 3\varphi - d_{11}\cos 3\varphi)\,\sigma_+$
$3m$	$d_{22}\cos 3\varphi$	$[(d_{22}\sin 3\varphi\cos\theta - d_{15}\sin\theta)^2 + \gamma^2(d_{22}\sin 3\varphi\sin\theta + d_{15}\cos\theta)^2]^{1/2}$
32	$d_{11}\sin 3\varphi$	$d_{11}\sigma_+\cos 3\varphi$
3	$d_{11}\sin 3\varphi + d_{22}\cos 3\varphi$	$[(d_{22}\sin 3\varphi\cos\theta - d_{11}\cos 3\varphi\cos\theta - d_{15}\sin\theta)^2 + \gamma^2(d_{22}\sin 3\varphi\sin\theta - d_{11}\cos 3\varphi\cos\theta + d_{15}\cos\theta)^2]^{1/2}$
$\bar{4}3m$, 23 / $\bar{4}2m$	0	$d_{14}\sigma_-\sin 2\varphi$
$\bar{4}$	0	$(d_{15}\cos 2\varphi + d_{14}\sin 2\varphi)\,\sigma_-$

$\sigma_+ = (\cos^2\theta + \gamma^2\sin^2\theta)^{1/2}$, $\sigma_- = (\sin^2\theta + \gamma^2\cos^2\theta)^{1/2}$, $C = (1+\gamma^2)^{-1/2}$

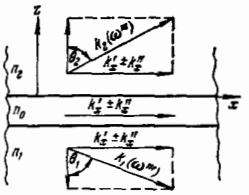

FIG. 18

frequency is $n_{\pm}^* = 0$. In the case of excitation of waves of equal type and frequency in the same direction, the effective index for the nonlinear polarization of the second harmonic coincides with n* for the first-harmonic waves.

The field excited by the nonlinear-polarization wave can be represented as a sum of surface waves and radiation waves:

$$E(x, z) = E_{\text{rad}}(x, z) + \sum_m C_m E_m(x, z);$$

here C_m are the surface-wave amplitudes.

By varying the film thickness and the propagation direction of the initial waves it is possible to obtain surface waves and radiated waves at the combination frequencies. The energy transfer into the combination-frequency wave is effective if n* for one of the waveguide modes at the frequency $\omega''' = \omega' \pm \omega''$ coincides with the effective refractive index for the nonlinear-polarization wave: $n^*(\omega''') = n_{\pm}^*(\omega''')$. As already noted, in the case of three-particle interaction in a nonlinear waveguide the synchronism condition can be satisfied by choosing the film thickness and the type of the wave for each frequency. However, the efficiency of excitation of combination frequencies is determined not only by the wave synchronism, but also by the extent to which the distribution of the nonlinear-polarization wave at the combination frequency agrees with the distribution of the field of the initial waves. This in turn is governed by the choice of the types of modes and orientations of the nonlinear dielectric in the film.

Excitation of radiation waves at combination frequencies becomes possible in a film waveguide when the condition $n_{\pm}^* < n_1(\omega' \pm \omega''), n_2(\omega' \pm \omega'')$ is satisfied. If the waveguide is assumed to be infinite along the x axis, then the optical field in the boundary dielectrics constitutes plane waves radiated at angles θ_1 and θ_2 (Fig. 18), with $\sin\theta_{1,2} = n^*(\omega' \pm \omega'')/n_{1,2}(\omega''')$. In the case of the already mentioned opposite propagation of the

initial waves with equal frequency, ($\omega' = \omega'' = \omega$, $\omega' + \omega'' = 2\omega$, $n^{\pm}_{\pm}(2\omega) = 0$, an in-phase distribution of the nonlinear-polarization wave is realized at the second-harmonic frequency. This polarization excites two plane waves in a direction normal to the waveguide surface, and the excitation of the plane wave at the second-harmonic frequency takes place at arbitrary film thicknesses. The radiation waves can be realized by propagation of the initial waves in one direction, if $n^{\pm}_{\pm}$ is smaller than the refractive index of the boundary dielectric at the combination frequency, but larger than the refractive indices of the same dielectric at the frequencies ω' and ω''.

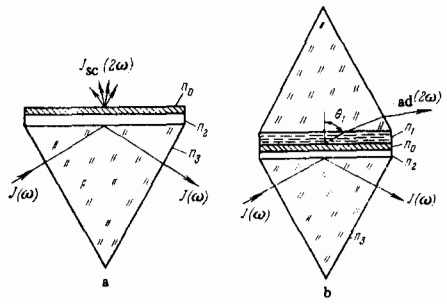

FIG. 19

Excitation of surface waves at combination frequencies is the most effective, since the output power is proportional in this case to the square of the length of the nonlinear waveguide. This regime can be realized if the waveguide is transparent enough at all the interacting frequencies and if the synchronism conditions are satisfied. To satisfy the latter requirement, the calculated waveguide thickness (h) should be maintained accurate to $\Delta h/\lambda \sim \lambda/l$, where l is the interaction length. It is difficult to attain this in practice at present.

It is easy to obtain radiated waves at combination frequencies, since this case is less critical to variation of the film thickness. In addition, it is permissible to use films with attenuation at the combination frequency, since the energy of the wave at this frequency is extracted from the waveguide over lengths on the order of the film thickness. The main shortcoming of generation of radiation waves is its low efficiency, since the output power is proportional to the length of the waveguide.

A promising possibility for the observation of nonlinear effects is afforded by the use of single-crystal $LiNbO_3$ film in a quartz substrate [11]. The axis of the $LiNbO_3$ crystal should be oriented perpendicular to the film plane. If the second harmonic is obtained by using the $H_1(\omega)$ and $E_1(2\omega)$ modes, then the nonlinear transformation is determined by the nonlinear interaction constant d_{31}. At a pump wavelength $\lambda = 1.06\ \mu$, the thickness of the $LiNbO_3$ film should be approximately $2.5\ \mu$.

In the experiment, nonlinear thin-film waveguides were used to obtain the second harmonic of a neodymium-glass laser [29]. The system consisted of a prism (TF-5) an LiF_2 film as the optical gap, and a ZnS film as the waveguide layer (Fig. 19a). The optical-gap thickness was chosen such that the Q of the waveguide was determined mainly by the coupling and not by the film loss. The second harmonic ($\lambda = 0.53\ \mu$) was seen at the resonant incidence angle as a bright green spot–spatially-incoherent radiation.

To obtain spatially-coherent radiation waves at the second harmonic, the system was modified somewhat, namely, nitrobenzene (n_1) was placed over the waveguide layer (Fig. 19b). The thickness of the ZnS waveguide layer was chosen such that the phase velocity of the excited first-harmonic wave exceeded the phase velocity of the second-harmonic plane waves in the boundary medium (nitrobenzene). In this case the second-harmonic radiation angle was given by the expression $\sin\theta_1 = n^*(\omega)/n_1(2\omega)$. At an Nd-laser pulse power 20 kW, the efficiency of conversion in the polycrystalline ZnS film was 10^{-6}. The dependences of the power and of the second-harmonic radiation angle in nitrobenzene on the thickness of the waveguide layer were determined and compared with the calculations for the $E_2(\omega)$ mode.

Generation of surface waves at the second harmonic in a thin film was obtained in [52]. The nonlinear waveguide was a chemically-polished GaAs plate with cross section $3.2 \times 160\ \mu$. Radiation from a CO_2 laser was introduced through the end face of the plate with the aid of a lens. The range of second-harmonic generation corresponded to the rotational lines of the CO_2, which lie between 9.2 and 10.8 μ without tuning of the nonlinear crystal. The broad phase-matching band is due, on the one hand, to the nature of the phase matching in thin films, and on the other to the inhomogeneity of the waveguide thickness along the ray trajectory. The low conversion efficiency ($\sim 10^{-2}$) was due, first, to the low powers of the energy input due to the low crystal-damage crystal, and second to the inefficient method of introducing the light ray through the end face. To obtain the second harmonic in thin-film waveguides it is also possible to use the nonlinear properties of the substrate. In [51] they investigated an optical waveguide of polycrystalline ZnS film, deposited on a single-crystal ZnO substrate. The surface wave in the film was excited by a Nd^{3+}:YAG laser, and the field penetrating into the substrate produced in it a nonlinear-polarization wave at the second-harmonic frequency. The thickness of the ZnS film was chosen such that the nonlinear-polarization wave propagated in the substrate with a higher velocity than the velocity of light in the substrate. The second-harmonic radiation was observed in the form of Cerenkov radiation at an angle $\theta_1 = \sin^{-1}[n^*(\omega)/n_2(2\omega)]$.

5. CONVERSION OF SURFACE WAVES

Thin-film optical waveguides can be used not only for frequency conversion of surface waves (see Chap. 4), but also for spatial scanning of the waves. As in the case of volume crystals, a promising method is the acoustic method, namely the interaction of light with elastic waves propagating in the film. The possibility of obtaining large concentrations of optical and acoustic energy in thin films gives grounds for hoping that effective film spatial modulators can be developed.

The interaction between acoustic and surface optical waves in a thin-film waveguide can be studied analytically by using the perturbation method [53]. For simplicity, a symmetrical dielectric waveguide ($n_1 = n_2 = 1$) is considered, in which the change of the dielectric constant, due to the acoustic wave, is represented in the form

$$\varepsilon = \begin{cases} n_0^2[1 - p\cos(Kx - \Omega t)], & |z| \leqslant h/2, \\ 1, & |z| > h/2, \end{cases} \qquad (5.1)$$

where p is the amplitude of the change of ϵ/ϵ_0 ($p \ll 1$).

We assume that an antisymmetrical type-H_m light wave propagates collinearly with the acoustic wave, and write down the y component of its dielectric vector in the form

$$E^{(i)}_{y,m} = C^m_0 \sin\left(\sqrt{n_0^2 - n_m^{*2}}\,kz\right) \exp\left[i\left(n^*_m kx - \omega_i t\right)\right], \qquad |z| \leqslant h/2,$$

$$E^{(i)}_{y,m} = \pm\, C^m_0 \sin\left(\sqrt{n_0^2 - n_m^{*2}}\,kh\right) \times \exp\left[-k\sqrt{n_m^{*2} - 1}\left(|z| - \frac{h}{2}\right)\right] \exp\left[i\left(n^*_m kx - \omega_i t\right)\right], \qquad \pm z > h/2. \tag{5.2a, 5.2b}$$

Here C_0^m is a constant and n^*_m is the root of the dispersion equation of the symmetrical waveguide (see (1.13) with $n_1 = n_2 = 1$).

We obtain the solution of the wave equation for the film in the surrounding medium:

$$\frac{\partial^2 E_y}{\partial x^2} + \frac{\partial^2 E_y}{\partial z^2} - \frac{n_0^2}{c^2}\frac{\partial^2 E_y}{\partial t^2} = \frac{n_0^2}{c^2}\, p \cos\left(Kx - \Omega t\right) \frac{\partial^2 E_y}{\partial t^2}, \qquad |z| \leqslant \frac{h}{2}, \tag{5.3a}$$

$$\frac{\partial^2 E_y}{\partial x^2} + \frac{\partial^2 E_y}{\partial z^2} - \frac{1}{c^2}\frac{\partial^2 E_y}{\partial t^2} = 0 \qquad |z| > \frac{h}{2}. \tag{5.3b}$$

The right-hand side of (5.3a) is the perturbation introduced by the acoustic wave. The solution of these wave equations can be represented in the form of the sum of the incident wave and the scattered waves

$$E_y = A^{(i)} E^{(i)}_{y,m} + \sum_l A_l^{(s)}(x)\, E_{y,l}(x, z, t;\, \omega_s) + \int_0^h q(\xi, x)\, E_y(\xi;\, x, z, t;\, \omega_s)\, d\xi. \tag{5.4}$$

The functions $E_y(\xi; x, z, t; \omega_S)$ describe radiated modes,

$$E_y(\xi;\, x, z, t;\, \omega_s) = \begin{cases} B \sin k_z z \cdot \exp\left[i\left(k_x x - \omega_s t\right)\right], & |z| \leqslant h/2, \\ \left(Ce^{i\xi z} + \overline{C}e^{-i\xi z}\right) \exp\left[i\left(k_x x - \omega_s t\right)\right], & |z| > h/2; \end{cases} \tag{5.5}$$

where $k_X = \sqrt{k^2 - \xi^2}$ and $k_Z = \sqrt{n_0^2 k^2 - k_X^2}$.

The principal task is to determine the function $q(\xi, x)$, which is due to the right-hand side of (5.3a). Substituting the value of E_y from (5.4) in (5.3a) and equating terms belonging to the same order of the perturbation, and also integrating the right-hand and left-hand sides with respect to z from zero to ∞, we obtain the following results [53]:

When the propagation directions of the acoustic and optical waves coincide, the function $q(\xi, x)$ is maximal if the conditions $\omega_S \approx \omega_i - \Omega$ and $k_X \approx \pm(n^*_m k - K)$ are satisfied. In the case of propagation in opposite directions, $q(\xi, x)$ is maximal at $\omega_S \approx \omega_i + \Omega$ and $k_X \approx \pm(n^*_m k - |K|)$. The variation of the radiation angle $(\Delta\theta)$ is connected with the change of the acoustic frequency (Δf) by the relation $\Delta\theta = \lambda \Delta f/(\sin\theta)\cdot V$, where V is the phase velocity of the acoustic wave. An analysis carried out for a GaAs waveguide and $\lambda = 10.6\ \mu$ has shown that in this case, for a beam inclination $\Delta\theta \approx 0.45$ rad ($\Delta F \approx 50$ MHz) it is necessary to have an acoustic energy lower by one order of magnitude than in the case of a three-dimensional acoustic deflector with similar characteristics.

One of the problems connected with the interaction between elastic and optical waves in thin films is the excitation of acoustic oscillations in the optical waveguide. Up to now, the experiments were performed with acoustic surface waves excited in a piezoelectric by opposing-post converters. These waves in turn excited surface waves in a film coated in the piezoelectric crystal. The short-comings of this method are obvious. To obtain an optical waveguide it is necessary to use a substrate with a refractive index smaller than n_0 of the film. The most widely used films, glass and organic,

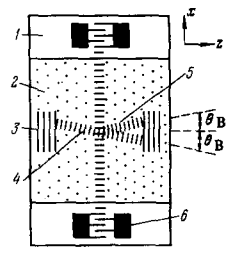

FIG. 20

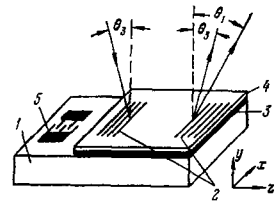

FIG. 21

have $n_0 \approx 1.5$; consequently, the substrate should have an even smaller refractive index n_1. However, piezoelectrics with small n_1 have small electroacoustic constants and small elastic-wave excitation efficiencies. In the case of substrates of $LiNbO_3$ crystals ($n_1 \approx 2.2$), a metal layer is deposited on the substrate in order to maintain the waveguide properties of the glass films, followed by a dielectric film. But in this case the metal introduces additional losses in the waveguide and increases the surface-wave attenuation.

The authors of [54] have demonstrated experimentally the deflection of the light beam interacting with an acoustic wave in an optical waveguide. The scanning was carried out in the plane of a glass film sputtered on α-quartz, in which surface acoustic waves were excited. The light flux propagated relative to the acoustic wave at the Bragg-scattering angle $\theta_B = \sin^{-1}(\lambda_0/2\Lambda)$, where $\lambda_0 = 2\pi/n_0 k$ is the wavelength of the light on the film, and Λ is the length of the acoustic wave. The scattered ray was deflected from the principal ray through an angle $2\theta_B$, which amounted to $\approx 1.3°$ in this experiment. The deflection efficiency was $\approx 66\%$.

The scattering of optical surface waves by acoustic waves in collinear propagation was investigated experimentally in [55], and a redistribution of the energy among the modes was observed. This effect is the analog of the Bragg scattering of light by elastic waves in anisotropic bulky media, except that to obtain phase matching in parametric excitation in thin films there is no need to use anisotropic materials (see Chap. 4). The waveguide substrate was single-crystal $LiNbO_3$ (one in Fig. 21), on which an aluminum layer 3 was deposited, followed by a glass film 4 (the number 5 in Fig. 21 denotes the converter for the surface acoustic modes). An He-Ne laser excited the H_1 mode in the film through a diffraction input unit 2; the energy of the H_1 mode was transferred by the interaction with the acoustic surface wave to the mode H_2, which was extracted from the film at an angle θ_1 that differed by ~4° from the angle θ_3 of the mode H_3. The conversion efficiency was 55% and was determined principally by the overlap integral:

$$\tau = \frac{\int_{-\infty}^{+\infty} v_a(z)\, v_1(z)\, v_3(z)\, dz}{\int_{-\infty}^{+\infty} v_a^2(z)\, dz \int_{-\infty}^{+\infty} v_1^2(z)\, dz \int_{-\infty}^{+\infty} v_3^2(z)\, dz}, \tag{5.6}$$

where $v_1(z)$ and $v_3(z)$ are the distribution functions of the E_y components for the modes H_1 and H_3, and

$$v_a(z) = \begin{cases} 1, & 0 \leqslant z \leqslant h, \\ 0, & z \geqslant h \end{cases}$$

is the distribution function of the stress produced by the acoustic wave. In this case, the nonlinear polarization excited by one of the modes does not coincide with the other mode, this resulting in a small value $\tau \approx 0.027$ and a low conversion efficiency. The overlap integral

can be increased by choosing a more suitable distribution of the acoustic energy (e.g., asymmetrical) or by using an asymmetrical waveguide with appropriate modes.

The acoustic method of surface-wave mode conversion is not the only one. As indicated in Chap. 4, when surface waves propagate in an anisotropic waveguide, their polarization changes continuously, and this produces automatically scattering of light over different oscillation modes. The polarization can vary also in an isotropic film if the boundary media from which the light rays are reflected are anisotropic or gyrotropic. The surface-wave field that penetrates into the boundary media is given by

$$Ce^{-\gamma k|z|}\exp[i(n^*kx-\omega t)],$$

where $\gamma=\sqrt{n^{*2}-n^2}$ is the damping constant. For an anisotropic substrate, there exist two eigenvalues γ_1 and γ_2 of the damping constant. Inasmuch as in the general case these two natural modes in the substrates are not purely transverse or purely longitudinal, it follows from the boundary conditions that the E_m and H_m modes in the film are likewise not purely transverse or purely longitudinal. Thus, when rays are reflected from the boundary between the film and the anisotropic medium, energy is transferred from one mode to another. In order for this conversion effect to accumulate, it is necessary to obtain a degenerate propagation of the surface waves, in which the same phase shifts are obtained upon reflection of the E_m and H_m modes. Usually when light is reflected from isotropic dielectrics at one and the same angle, the phase shifts for different polarizations are different, but by using suitable anisotropic media as boundary media it is possible to obtain degenerate propagation.

In [56], a theoretical analysis was carried out of the conversion of optical modes in films with anisotropic boundary media, and the coherence lengths were calculated numerically for different films, anisotropic and gyrotropic substrates, and boundary media. The possibility of obtaining 100% conversion was demonstrated, and the permissible deviations of the film thicknesses and of the mode-excitation angles from their optimal values were estimated. The indicated conversion principle was realized in [86]. The optical waveguide was made up of a glass film sputtered on glass having a smaller refractive index. The film thickness was such that only the two lower modes H_1 and E_1 could be excited. A gas laser ($\lambda=0.63\ \mu$) was used to excite the H_1 mode. To obtain conversion, a suitably oriented plate of crystalline quartz was pressed against the film (until optical contact was obtained). H_1 and E_1 modes were observed in the output. The efficiency of conversion of H_1 into E_1 was ≈15%.

6. AMPLIFICATION AND GENERATION OF LIGHT IN THIN FILMS

The principle of miniaturization of optical circuits, which have found their way in modern communication technology, computer technology, etc., has raised the question of development and production of film amplifiers and light generators. The possibility of amplifying surface waves in a flat dielectric waveguide was first demonstrated theoretically in [59], where the active medium considered was gas adjacent to a waveguide. By now, a large number of active elements in thin-film waveguides was proposed and realized in practice. In particular, in [60] there was reported amplification of light of wavelength $\lambda=6328$ Å in a polyurethane film activated by rhodamine B dye. The waveguide film was obtained by immersing a clean glas substrate (microslide) into a specially prepared solution of two components of polyurethane resin and dye, followed by drying of the slide in a vertical position in air and in an oven. The rhodamine-B concentration in the film was 7.5×10^{3} mole/liter (film No. 1) and 3.3×10^{-2} mole/liter (film No. 2). The film had a refractive index $n_0=1.55$ and the substrate had $n_1=1.51$. The film was pumped with a nitrogen laser of power ≈43 kW and pulse duration 6.6 nsec. The laser radiation was focused into a line 28 mm long and 0.3 mm wide. In the absence of feedback, superradiance was observed in the dye-activated film. A polarization analysis of the radiation extracted from the film with the aid of a rutile prism revealed the presence of H_m and E_m waves in the radiation. The superradiance pulse duration, 5.6 nsec, was shorter than the pump pulse. The emission spectrum was broad enough, $\Delta\nu\approx200$ A, and the center of the emission band was at $\lambda=6320$ Å. Amplification of light in a film activated with rhodamine B was also demonstrated in [60]. To this end, radiation from an He-Ne laser ($P_i=0.15$ mW) was introduced into the film and extracted from it by means of prisms separated by a distance of 16 mm. The output radiation was analyzed with a spectrometer and registered with a photomultiplier on an oscilloscope.

It was established that when the power incident on the input prism is increased, the gain decreases, saturation being observed in the region of large P_i. The maximum gain was 12.5 cm^{-1} for film No. 2 and 8.4 cm^{-1} for film No. 1. An investigation of the dependence of the gain on the nitrogen-laser power P_{N_2}, performed on film No. 1, has shown that when the pump power P_{N_2} increases the gain increases. However, at sufficiently high pump levels ($P_{N_2}>14$ kW/cm) the gain exhibits saturation, and for smaller P_i the gain is higher in the saturation region. We note that no superradiance was observed when the pump power was reduced to 10 kW/cm, although an appreciable gain of the He-Ne laser light was registered by the receiving apparatus.

An interesting design of a film-type light amplifier was obtained in [65]. Using the penetration of the field of a surface wave propagating in a film into the boundary medium, the authors chose one of these media to be the dye rhodamine 6Zh. The dye was pumped by a surface wave from an external source, excited in the film with the aid of a prism. An important factor in such an amplifier is the proper choice of the refractive indices of the film, substrate, and dye solution, so as to ensure the largest penetration of the pump field and of the amplified field into the dye. Obviously, the optimal case will correspond to a dye-solution refractive index close to the refractive index of the film. The authors of [65] deposited on the film a rhodamine 6Zh solution with concentration 3×10^{-3} mole/liter and pumped it with the second harmonic of a Nd^{3+}:YAG laser. At low pump levels they observed spontaneous emission of the dye in the waveguide, and at large concentration they observed superradiance with wavelength $\lambda=5900$ Å emerging from the output prism. Estimates show that the gain necessary to observe superradiance should reach e^{20}.

Progress in the technique of sputtering glass films has made it possible recently to obtain a glass film activated with Nd^{3+} ions and having very low losses (0.05

dB/cm for the fundamental mode) [66]. A film amplifier for light of wavelength 1.06 μ was realized in [66] on the basis of such a film. The activated film ($n_0 = 1.55$, 3.5 wt% Nd), deposited on a glass substrate with $n_1 = 1.53$, was illuminated by a xenon flash lamp. The light beam from a cw Nd^{3+}:YAG laser was introduced into the film and extracted from it with the aid of prisms. The distance between prisms was 5 cm, and the length of the illuminated region was 3 cm. At a pump energy 130 J, a 16% gain per pass was registered. A study of the dependence of the gain on the pump energy and on the power of the radiation amplified in the film has shown that it increases linearly with increasing pump (up to 200 J), and decreases linearly with increasing power of the light beam entering the film.

The necessary stage in the development of film lasers is the realization of an effective feedback in the film. The first step in this direction was made in [62], where generation was investigated in a periodic structure in which the feedback was provided by backward Bragg scattering of the light. The light was scattered by periodic spatial changes of the refractive index or of the gain of the amplifying medium itself. The changes of the refractive index n and of the gain α are given in the form

$$n(x) = n + \delta n \cos Kx, \quad \alpha(x) = \alpha + \delta\alpha \cos Kx, \tag{6.1}$$

where the x axis is directed along the optical axis and $K = 2\pi/\Lambda$. Here Λ is the period of the spatial modulation, and δn and $\delta\alpha$ are its amplitudes. A distributed-feedback laser of this type will emit light of wavelength λ determined by the Bragg condition (3.26)

$$\lambda = 2n\Lambda. \tag{6.2}$$

An expression was obtained in [62] for the threshold and for the spectral width of the simulated emission in such a periodic structure, on the basis of an analysis of the structure by the coupled-wave method (see Chap. 3). The condition under which generation sets in at large values of the gain $G = e^{2\alpha L}$, where L is the length of the periodic structure, is of the form

$$4\alpha^2 G^{-1} = \left(\frac{\pi\delta n}{\lambda}\right)^2 + \frac{(\delta\alpha)^2}{4}. \tag{6.3}$$

If only the refractive index of the medium is modulated, then the threshold condition reduces to

$$\delta n = \frac{\lambda \ln G}{L\pi\sqrt{G}}. \tag{6.4}$$

When the gain is double the threshold value at the center of the band, the threshold condition is satisfied for a spectral band $\Delta\lambda$, the width of which is given by

$$\frac{\Delta\lambda}{\lambda} = \frac{\lambda \ln G}{4\pi nL}. \tag{6.5}$$

To illustrate the foregoing relations, let us assume that the amplifying medium has a length L = 10 mm, a gain G = 100, and an emission wavelength $\lambda = 0.63$ μ. Equation (6.4) indicates that generation will take place if $\delta n \geq 10^{-5}$. For the width of the radiation band we obtain from (6.5) the value $\Delta\lambda \approx 0.1$ Å. A laser with distributed feedback was experimentally realized using dye in a gelatin film. The laser length was 10 mm and the width was 0.1 mm. The film was deposited on a glass substrate. Gelatin sensitized with ammonium bichromate $(NH_4)_2Cr_2O_4$ was exposed to two coherent beams from an He-Cd laser. The interference pattern produced with such an illumination of the gelatin had a period of 0.3 μ. The gelatin was then developed by the method used in holography [37,38,69], with a resultant spatial modulation of the refractive index. The developed gelatin was immersed in a solution of rhodamine 6Zh, to permit the dye to penetrate into the pores of the gelatin layer. After drying, a structure with distributed feedback was obtained, and was illuminated with ultraviolet radiation from a nitrogen laser. At pump densities higher than 10^6 W/cm^2, generation with wavelength 0.63 μ was observed. An analysis of the emission spectrum of the film laser, with the aid of a spectrometer, has shown that the line width is smaller than 0.5 Å. The line width of the stimulated luminescence of the rhodamine 6Zh in a homogeneous gelatin film, under the same pumping conditions, was 50 Å, and the center of the line was at the wavelength $\lambda = 0.59$ μ. Thus, the presence of distributed feedback led to an appreciable narrowing of the radiated line. Lasing in gelatin films of different thicknesses and under different pumping conditions was investigated. In addition to the possibility of obtaining single-frequency generation in a film $h \approx 14\mu$ thick, it was noted that multifrequency generation is possible at larger pumps and in thicker films. The multifrequency character of the radiation is due to generation of different modes of the gelatin film.

Variation of the period of the spatial modulation of the refractive index or of the gain makes it possible to obtain tunable radiation from a laser with distributed feedback. To this end one can use the well known property of organic dye solutions, namely that the gain and refractive index are altered by absorption of intense optical radiation. A tunable thin-film laser was produced in [67] using a polyurethane waveguide film activated with rhodamine 6Zh and pumped with two interfering coherent light beams (Fig. 22). Depending on the angle 2θ between them, the radiation wavelength λ_L varied in accordance with the formula

$$\lambda_L = \frac{\lambda_p n^*}{q_B \sin\theta}$$

where q_B is the order of the Bragg scattering (see Chap. 3). The pump was the second harmonic of a ruby laser with $\lambda_p = 0.347$ μ. The line width of the film laser did not exceed several tenths of an Angstrom unit at high pump levels. The possibility of constructing a laser based on the foregoing principle is apparently limited to media with large gains.

The development of a thin-film ring laser, in which strong feedback is easiest to obtain, can increase the class of thin-film generators, by making possible the use of media with moderate gains.

A film ring laser was realized in [63] by depositing an activating film on the surface of a cylindrical glass rod. The optical path of the light in the film followed the periphery of the rod. The pump was a nitrogen laser

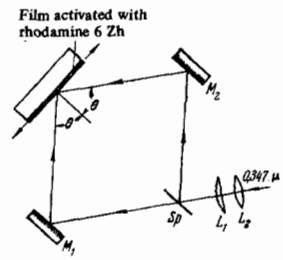

FIG. 22

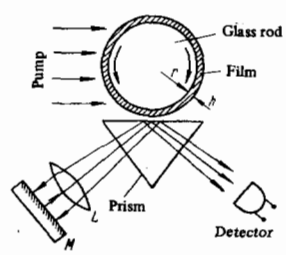

FIG. 23

($\lambda = 3371$ Å), the output beam of which illuminated a narrow strip of the film on the rod. The light generated in the film was extracted from it with the aid of a prism (Fig. 23). Inasmuch as the light propagates in the annular film in two directions, two output beams were observed. These rays were well collimated in the vertical direction (along the rod), since the height of the pumped region was ≈0.2 mm. In the horizontal direction, they have an angle spread ~1° at a rod diameter $2r = 5$ mm. This spread is due to the finite spectral width of the laser light and to the curvature of the film. The film curvature leads to a very short length of the region of coupling with the output prism, and consequently to an angular broadening of the output beam. The width of the gap between the prism and the film can be optimized by regulating the pressure of the prism against the rod.

In the experiment, a polyurethane film activated with rhodamine 6Zh dye (8×10^{-3} mole/liter) was deposited on a glass rod ($n_1 = 1.47$). The film had a refractive index $n_0 = 1.55$ and a thickness 0.8 μ. Only the fundamental modes H_1 and E_1 could propagate in the film. Measurements of the output power as a function of the pump power have revealed a clearly pronounced threshold. The threshold pump power was 15 kW (1.5 MW/cm^2). However, only a small fraction of the light (~1 kW) incident on the film was absorbed in the film. The emission spectrum of the ring laser was quite broad and reached 110 Å, with a maximum at $\lambda = 6200$ Å. The spectrum has revealed the natural frequency of the ring-laser resonator, this being the most direct proof of the presence of feedback. The intermode distance in the wavelength scale is determined in the case of a ring laser by the relation

$$\Delta\lambda = \frac{\lambda^2}{2\pi r n_{gr}},$$

where $2r$ is the rod diameter, $n_{gr} = c/v_{gr}$, and v_{gr} is the group velocity of the wave in the film. An intermode distance $\Delta\lambda \approx 0.553$ Å was observed in the experiment in the case of a ring laser on a rod of diameter $2r = 1.397$ mm. This value agrees well with the theoretical value obtained for longitudinal modes of a film ring laser with $n_{gr} = 1.583$ and $h = 0.8$ μ. Similar measurements were performed for a laser on a rod of diameter $2r = 1.05$ mm.

As noted earlier, two beams are observed at the output of the ring laser. If a lens and a mirror are placed in the path of one of the beams, which is thereby returned to the film, it is possible to obtain a unidirectional ring laser. Such a film laser was realized experimentally in [68]. The maximum power ratio of the two output beams reached 17. Replacement of the mirror by a diffraction grating has made it possible to tune the center of the emission band of such a laser within a narrow range, by displacing the lens. It should be noted that a film ring laser can be coupled quite simply with a flat film on a substrate and used to introduce the radiation into the film.

An electroluminescence laser or a semiconductor laser can be used as a thin-film active element. A report of the first attempts to develop an electroluminescence laser was published in [69]. In that study, narrowing of the luminescence line was observed, together with a noticeable increase of the directivity of the radiation in a high-resistivity ($\rho \sim 10^8 - 10^{10}$ Ω-cm) ZnS semiconductor doped with manganese. The "threshold" values of the electric field intensity and of the current density through the sample reached $E \sim 1.4 \times 10^6$ V/cm and $j \sim 10^{-2}$ A/cm, respectively. The gain at the maximum of the luminescence band $\lambda_{max} = 5900$ Å turned out to be $(1-5) \times 10^3$ cm^{-1}. The mechanism for the production of inverted population in ZnSMn was impact excitation of the Mn^{2+} ions, as is evidenced, in the opinion of the authors, by the emission spectrum which is typical of the transition $^4T_1(^4G) \rightarrow A^6(^6S)$ in the Mn^{2+} ion, the low density of the threshold current, the absence of heating of the sample, and the large value of the internal quantum yield of the generation.

A suggestion that a semiconductor laser be used to excite thin-film waveguides is made in [70]. The idea of the proposed method is analogous to that described above in the discussion of an amplifier with an active medium adjacent to the film [65]. The only difference is that a semiconductor laser diode is used for pumping in this case.

The possibilities of using a semiconductor laser with a double heterostructure as an intense laser source directed coupled to a film waveguide were investigated in [71]. The authors believe that such a semiconductor laser can deliver a power on the order of 50 mW into the fundamental wave mode.

The use of electroluminescence and semiconductor lasers in optical integrated circuits is promising in view of their small dimensions, large efficiencies, and other advantages over lasers of other types.

[1)] Inasmuch as the main structural elements of this input device is a prism, it is frequently called a prism input.

[2)] This figure differs somewhat from Fig. 2 of [31] because we have used the opposite orientation of the x axis relative to the direction of the incident beam.

[1] L. N. Deryugin, A. N. Marchuk, and V. E. Sotin, Izv. Vuzov (Radioélektronika) 10, 134 (1967).
[2] V. I. Anikin, L. N. Deryugin, A. N. Marchuk, A. N. Osovitskiĭ, A. T. Reutov, and V. E. Sotin, Conf. on the Theory and Application of Dielectric waveguides in the Microwave and Optical Bands, Abstracts of Papers (in Russian), Moscow Power Inst., 1968.
[3] A. N. Marchuk and V. E. Sotin, Trudy, Lumumba Peoples' Friendship University, No. 23, 130 (1967).
[4] R. Shubert and J. H. Harris, IEEE Trans. MTT-16, 1048 (1968).
[5] S. E. Miller, Bell Syst. Tech. J. 48, 2059 (1969).
[6] P. K. Tien and R. Ulrich, J. Opt. Soc. Am. 60, 1325 (1970).
[7] J. E. Goell and R. D. Standley, Proc. IEEE 58, 1504 (1970).
[8] P. K. Tien, R. Ulrich, and R. J. Martin, Appl. Phys. Lett. 14, 291 (1969).
[9] A. S. Belanov, G. I. Ezhov, and V. V. Chernyĭ, in: Radioélektronika opticheskogo diapazona (Optical-Band Radioelectronics), Trudy VZMI, 1970, p. 3.
[10] A. S. Belanov and G. I. Ezhov, ibid., p. 18.
[11] P. K. Tien, Appl. Opt. 10, 2395 (1971).
[12] V. F. Vzyatyshev, G. D. Rozhkov, and A. N. Merkur'ev, Zarub. radioélektronika No. 12, 60 (1970).
[13] V. I. Anikin, ibid., No. 7, 111 (1971).
[14] J. Goell, K. Standley, and T. Li, Electronics 43 (18) 66 (1970); S. E. Miller, IEEE J. Quantum Electron. QE-8, 199 (1972).
[15] R. V. Pole, S. E. Miller, J. H. Harris, P. K. Tien, Appl. Opt. 11, 1675 (1972).
[16] D. Marcuse, Bell Syst. Tech. J. 48, 3187 (1969).
[17] D. Marcuse, ibid. 49, 273 (1970).

[18]J. M. Hammer, Appl. Phys. Lett. 18, 147 (1971).
[19]D. P. Russo and J. H. Harris, Appl. Opt. 10, 2786 (1971).
[20]R. Ulrich and R. J. Martin, ibid., p. 2077.
[21]R. Shubert and J. H. Harris, J. Opt. Soc. Am. 61, 154 (1971).
[22]L. N. Deryugin, A. N. Marchuk, and V. E. Sotin, Izv. vuzov (Radioélektronika) 13, 309 (1970).
[23]L. N. Deryugin, A. N. Marchuk, and V. E. Sotin, ibid. p. 974.
[24]J. H. Harris, R. Shubert, and J. N. Polky, J. Opt. Soc. Am. 60, 1007 (1970).
[25]R. Ulrich, ibid., p. 1337.
[26]J. E. Midwinter, IEEE J. Quantum Electron. QE-6, 583 (1970).
[27]F. Zernike and J. E. Midwinter, ibid., p. 577.
[28]V. I. Anikin, L. N. Deryugin, and V. E. Sotin, Izv. vuzov (Radioélektronika) 14, 371 (1971); J. E. Midwinter, IEEE J. Quantum Electron. QE-7, 345 (1971).
[29]V. E. Sotin, Candidate's dissertation (Moscow, 1969).
[30]J. H. Harris and R. Shubert, IEEE Trans. MTT-19, 269 (1971).
[31]R. Ulrich, J. Opt. Soc. Am. 61, 1467 (1971).
[32]P. K. Tien and R. J. Martin, Appl. Phys. Lett. 18, 398 (1971).
[33]M. L. Dakss, L. Kuhn, P. F. Heidrich, and B. A. Scott, ibid. 16, 523 (1970).
[34]H. Kogelnik and T. P. Sosnovski, Bell Syst. Tech. J. 49, 1602 (1970).
[35]D. B. Ostrovsky and A. Jacques, Appl. Phys. Lett. 18, 556 (1971).
[36]H. Kogelnik, Bell Syst. Tech. J. 48, 2909 (1969).
[37]T. Shankoff, Appl. Opt. 7, 2101 (1968).
[38]L. H. Lin, ibid. 8, 963 (1969).
[39]F. S. Chen, J. T. La Macchia, and D. B. Fraser, Appl. Phys. Lett. 12, 223 (1968).
[40]D. H. Close, A. D. Jacobson, J. D. Margerum, R. G. Brault, and F. J. McClumg, ibid. 14, 159 (1969).
[41]R. G. Brandes, E. E. Francois, and T. A. Shankoff, Appl. Opt. 8, 2346 (1969).
[42]D. Marcuse, Bell Syst. Tech. J. 48, 3233 (1969).
[43]D. H. Hensler, J. D. Cuthbert, R. J. Martin, and P. K. Tien, Appl. Opt. 10, 1037 (1971).
[44]J. E. Goell and R. D. Standley, Bell Syst. Tech. J. 48, 3445 (1969).
[45]J. H. Harris, D. R. Gia Russo, and R. Shubert, Proc. IEEE 59, 1123 (1971).
[46]P. K. Tien, G. Smolinsky, and R. J. Martin, Appl. Opt. 11, 637 (1972).
[47]V. F. Marchenko, Opt. Spektr. 21, 592 (1966); 22, 946 (1967).
[48]Y. Suematsu, Japan J. Appl. Phys. 9, 798 (1970).
[49]R. A. Andrews, IEEE J. Quantum Electron. QE-7, 523 (1971).
[50]V. F. Marchenko and V. K. Sotin, Abstracts of Papers of Fourth Symp. on Nonlinear Optics, (Kiev, 1968) (in Russian), Moscow Univ. Press, 1968.
[51]P. K. Tien, R. Ulrich, and R. J. Martin, Appl. Phys. Lett. 17, 447 (1970).
[52]D. B. Anderson, J. T. Blyd, ibid. 19, 266 (1971); D. B. Anderson and J. D. McMullen, Digest of Techn. Papers. Intern. Microwave Symposium, Dallas, 1969, p. 212.
[53]W. S. Chang, IEEE J. Quantum Electron. QE-7, 167 (1971).
[54]L. Kuhn, M. L. Dacs, P. F. Heidrich, and B. A. Scott, Appl. Phys. Lett. 17, 265 (1970).
[55]L. Kuhn, P. F. Heindrich, and E. G. Lean, ibid. 19, 428 (1971).
[56]Sh. Wang, J. D. Crow, and M. Shah, ibid., p. 187.
[57]Sh. Wang, M. Shah, and J. Crow, IEEE J. Quantum Electron. QE-8, 212 (1972).
[58]Sh. Wang, M. Shah, and J. Crow, J. Appl. Phys. 43, 1861 (1972).
[59]S. A. Raskutin, Radiotekh. i élektron. 15, 2527 (1970).
[60]M. S. Chang, P. Burlamacchi, C. Hu, and J. R. Whinnery, Appl. Phys. Lett. 20, 313 (1972).
[61]R. Ulrich and H. P. Weber, Appl. Opt. 11, 428 (1972).
[62]H. Kogelnik and C. V. Shank, Appl. Phys. Lett. 18, 152 (1971).
[63]H. P. Weber and R. Ulrich, ibid., p. 38.
[64]Digest of Technical Papers. Meeting on Integrated Optics, Las Vegas, 1972.
[65]E. P. Ippen and C. V. Shank, ibid., ThA1-1.
[66]H. Yajima, S. Kawase, and Y. Sekimoto, ibid., ThA9-1.
[67]J. E. Bjorkholm and C. V. Shank, ibid., ThA1-1.
[68]R. Ulrich, H. P. Weber, Appl. Phys. Lett. 20, 38 (1972).
[69]N. A. Vlasenko and Zh. A. Pukhlyĭ, ZhETF Pis. Red. 14, 449 (1971) [JETP Lett. 14, 306 (1971)].
[70]D. Z. Keune, N. Holonyak, R. D. Burnham, P. D. Dapkus, and R. D. Dupuis, Appl. Phys. Lett. 16, 18 (1970).
[71]J. Umeda, R. Ito, T. Tsukada, H. Nakajima, and O. Nakada, see [64], ThA7-1.
[72]F. Varsanyi, Appl. Phys. Lett. 19, 169 (1971).
[73]R. Ulrich, H. P. Weber, E. A. Chandross, W. J. Tomlison, and E. A. Franke, ibid. 20, 213 (1972).
[74]A. Yariv and R. C. Leite, ibid. 2, 55 (1963).
[75]O. S. Heavens, Optical Properties of Thin Solid Films, L., Butterworth Sci. Publ., 1955.
[76]D. F. Nelson and F. K. Reinhart, Appl. Phys. Lett. 5, 148 (1964).
[77]J. Hagashi, M. B. Ponish, and F. K. Reinhart, J. Appl. Phys. 42, 1929 (1971).
[78]E. Germaire, H. Stoll, A. Yariv, and R. G. Hunsperger, Appl. Phys. Lett. 21, 87 (1972).
[79]E. R. Schineller, R. Flam, and N. Wilmot, J. Opt. Soc. Am. 58, 1171 (1968).
[80]H. F. Taylor, W. E. Martin, D. B. Hall, and V. N. Smiley, Appl. Phys. Lett. 21, 95 (1972).
[81]H. W. Weber, R. Ulrich, E. A. Chandross, and W. J. Tomlinson, ibid. 20, 143.
[82]J. E. Goell, see [64], MB8-1.
[83]D. J. Channin, Appl. Phys. Lett. 19, 128 (1971).
[84]L. A. Vaĭnshteĭn, Élektromagnitnye volny (Electromagnetic Waves), Sov. Radio, 1957.
[85]M. Born and E. Wolf, Principles of Optics, Pergamon, 1966.
[86]M. Shah, J. Crow, and Sh. Wang, Appl. Phys. Lett. 20, 66 (1972).

Translated by J. G. Adashko